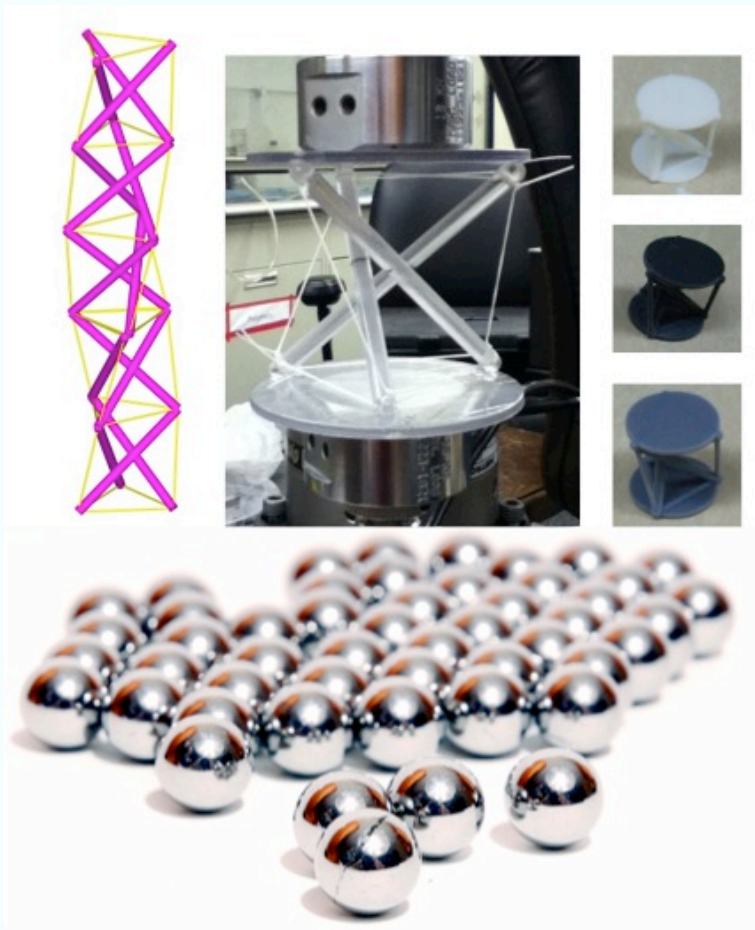


Wave Dynamics of Innovative Nonlinear Lattices

Fernando Fraternali

*Department of Civil Engineering
University of Salerno, Italy*

University of Augsburg
04 December 2014



Overview

Introduction

Part I: Basic Properties of Solitary Waves

Part II: Optimal Design of Granular Protectors

Part III: Solitary Waves on Tensegrity Metamaterials

Part IV: Concluding remarks / Future Work

Motivation

A novel area of research has emerged over the last few years regarding the design and manufacturing of structural lattices modulated with periodic elastic moduli and mass densities.

It has been shown that such linear elastic metamaterials may exhibit anomalous acoustic behaviors, like negative effective elastic moduli; negative effective mass density; acoustic negative refraction; phononic band gaps; and local resonance, to name just a few examples.

The dynamics of strongly nonlinear metamaterials with power-law interaction law between elements has also been investigated, revealing that elastically stiffening systems with power law exponent n greater than one (“normal” power-law materials) support compressive solitary waves and unusual reflection of wave on material interfaces.

Differently, elastically softening systems with $n < 1$ (“abnormal” power-law materials) support the propagation of rarefaction solitary waves under initially compressive impact loading.

The present talk focuses on the following features of the wave dynamics of granular and tensegrity metamaterials:

- Energy transport through solitary waves;
- Dependence of the wave profile on the material properties (t-lattices);
- Shock and impulse mitigation properties;
- Optimal design through Evolutionary Strategies;
- Practical applications.

Granular crystals are metamaterials composed of particles arranged in given geometrical configurations. Such systems are characterized by a highly nonlinear dynamics derived from the Hertzian contact interaction between particles and the zero tensile resistance between grains.

We optimize features of granular systems such as particle distribution, connectivity, size, and material properties. By designing granular protectors or containers optimally, the strongly nonlinear dynamics of granular systems can be exploited to produce fast decomposition of an external impulse into trains of solitary waves, energy trapping, and shock disintegration/reflection.

Concerning tensegrity structures, we explore their use as novel networks supporting energy transport through solitary waves. Experimental and theoretical studies have shown that the geometrically nonlinear response of tensegrity prisms may gradually change from stiffening to softening, depending on mechanical, geometrical and prestress variables. This extremely rich constitutive behavior can be dynamically tuned, by integrating control functions within the design of the structure.

We present theoretical and numerical results on the mechanics of periodic lattices of lumped masses connected by tensegrity prisms. The latter may exhibit either softening or stiffening elastic response tuned by local and global prestress.

The given results show that such systems are able to support tunable solitary rarefaction and compression waves and anomalous wave transmission and reflection between branches with different acoustic impedances.

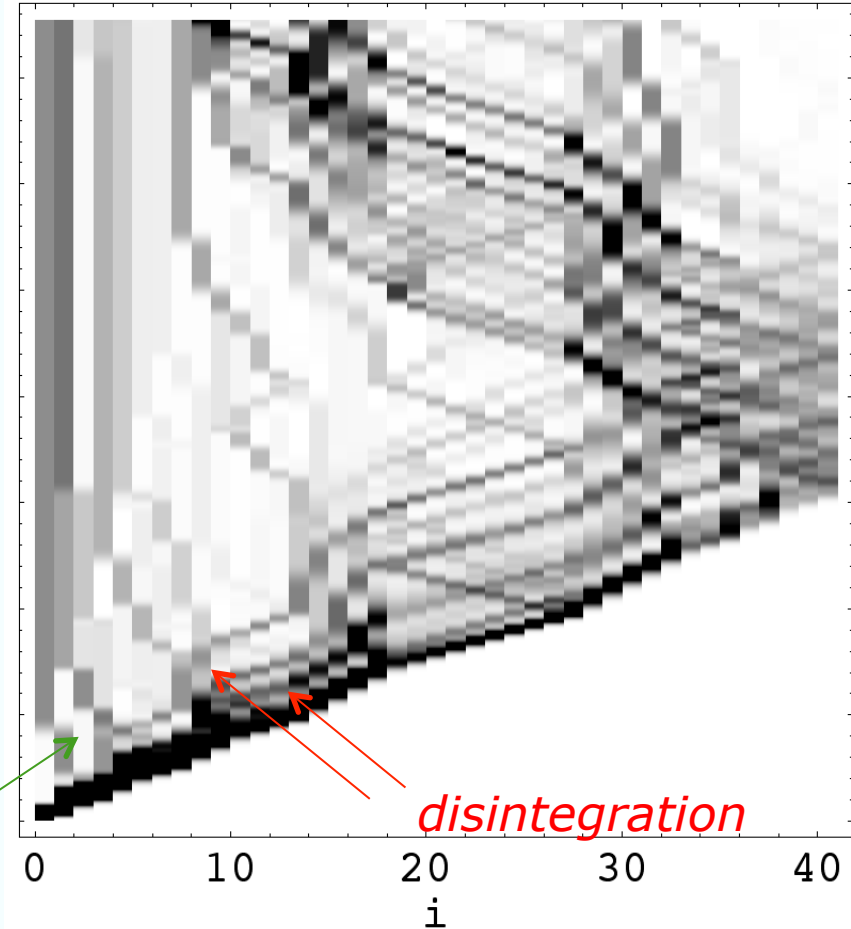
The observed behaviors pave the way to the optimal design of tunable tensegrity metamaterials, acoustic lenses, and innovative impact protection devices that do not require energy dissipation

Granular crystals

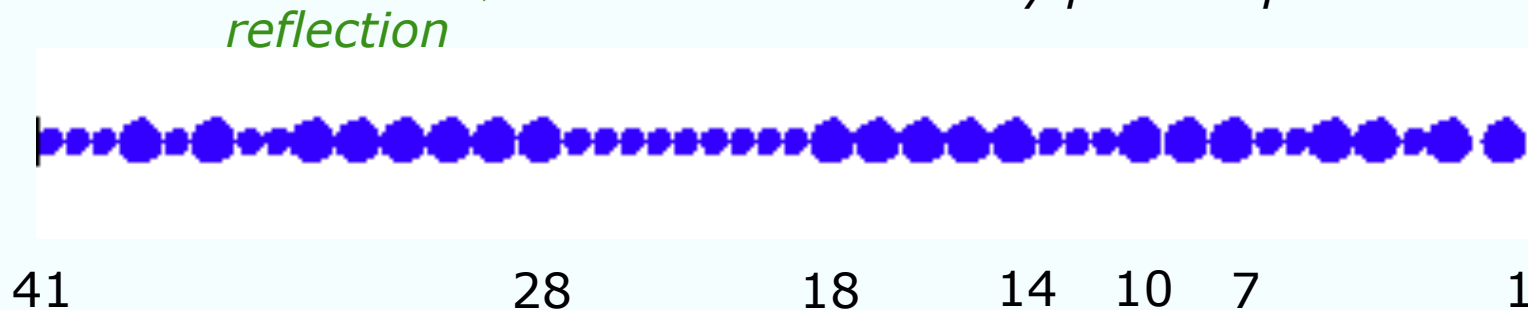
Two remarkable phenomena have been observed in the literature with reference to the wave dynamics of heterogeneous granular lattices:

a) disintegration of an incident pulse into a train of solitary waves when it passes from sections with **LARGE** radius to sections with **small** radius;

b) partial reflection in the opposite case (small \rightarrow **LARGE** transition)



Density plots of particle energies

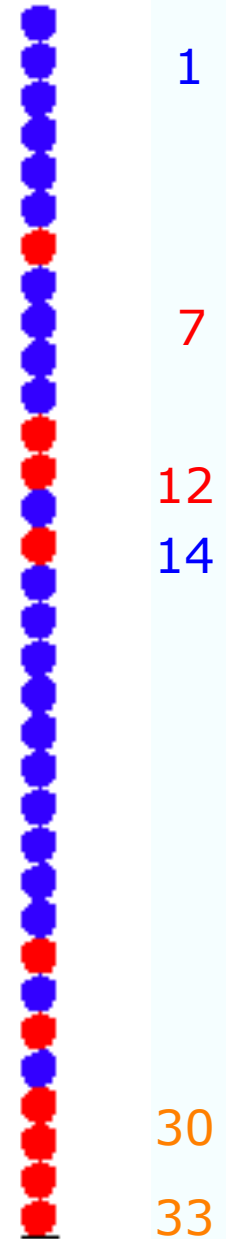
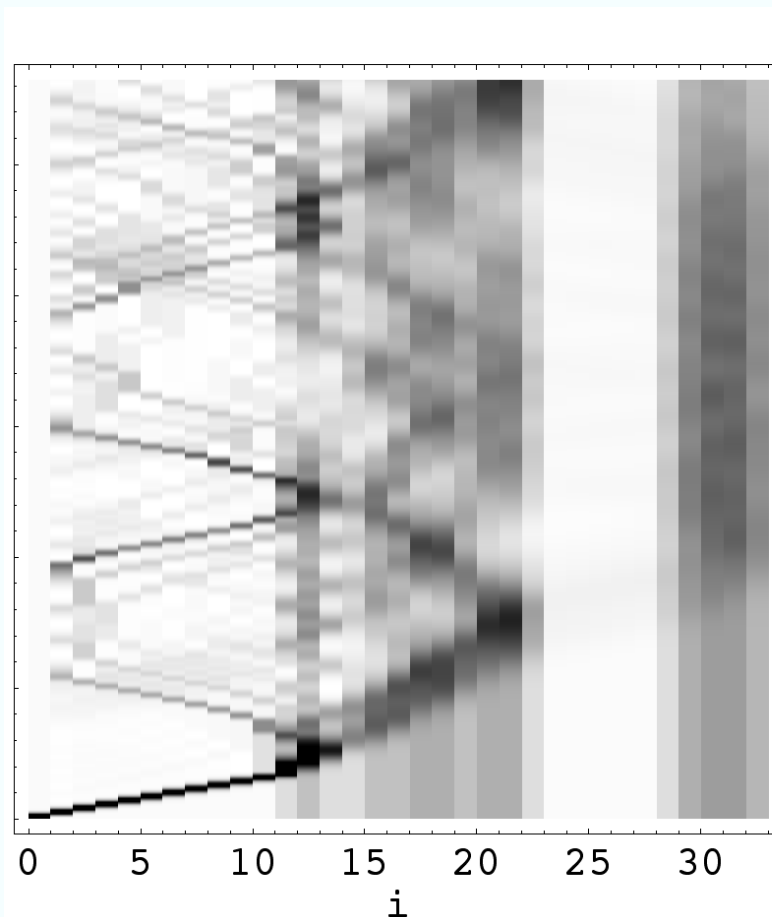


Similar behaviors have been observed at the interfaces between **soft** (e.g., rubber) and **hard** (e.g., steel) beads:

a) disintegration of an incident pulse into a solitary wave train when it passes from sections with **hard beads** to sections with **soft beads**;

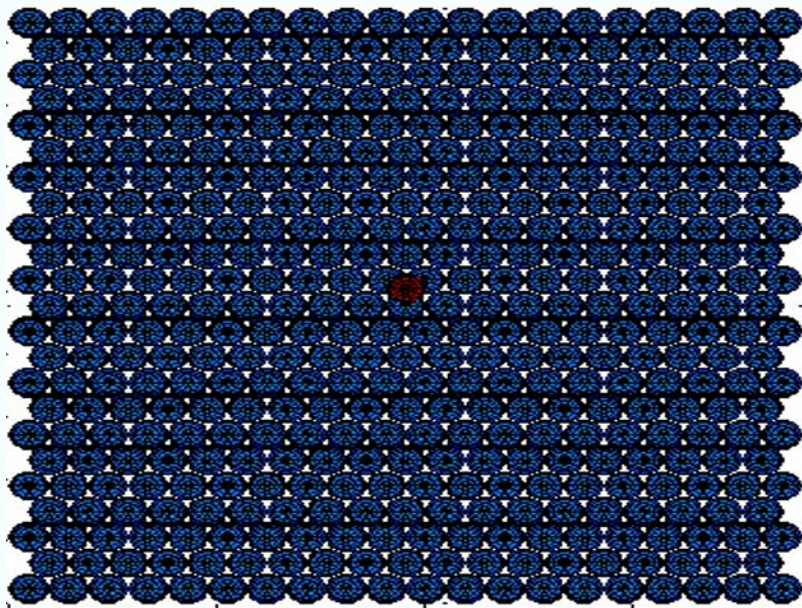
b) partial reflection in the opposite case (**soft** \rightarrow **hard** transition)

Density plot of particle energies

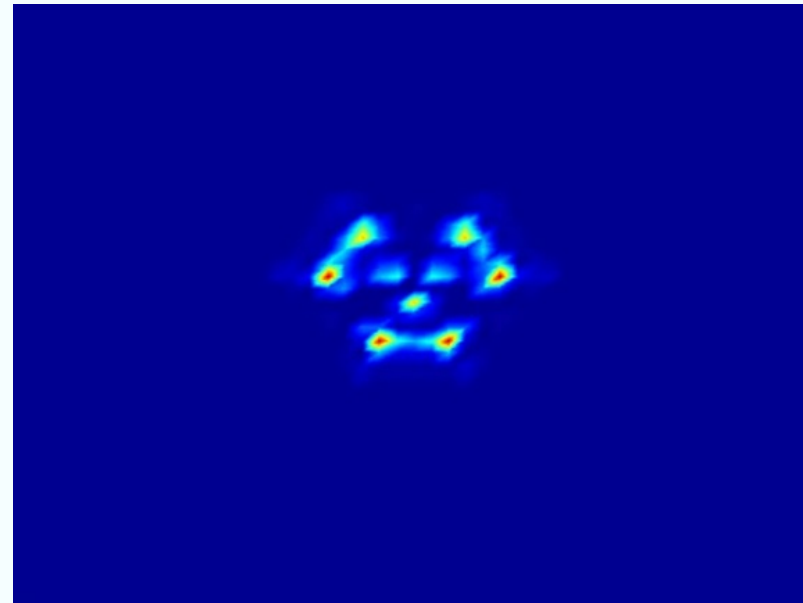


The previous 1D “*thermalization*” phenomena are accompanied by wave- redirection effects in 2D and 3D granular systems, leading to marked “energy- trapping” capability of the system (as opposed to energy dissipation).

animation >

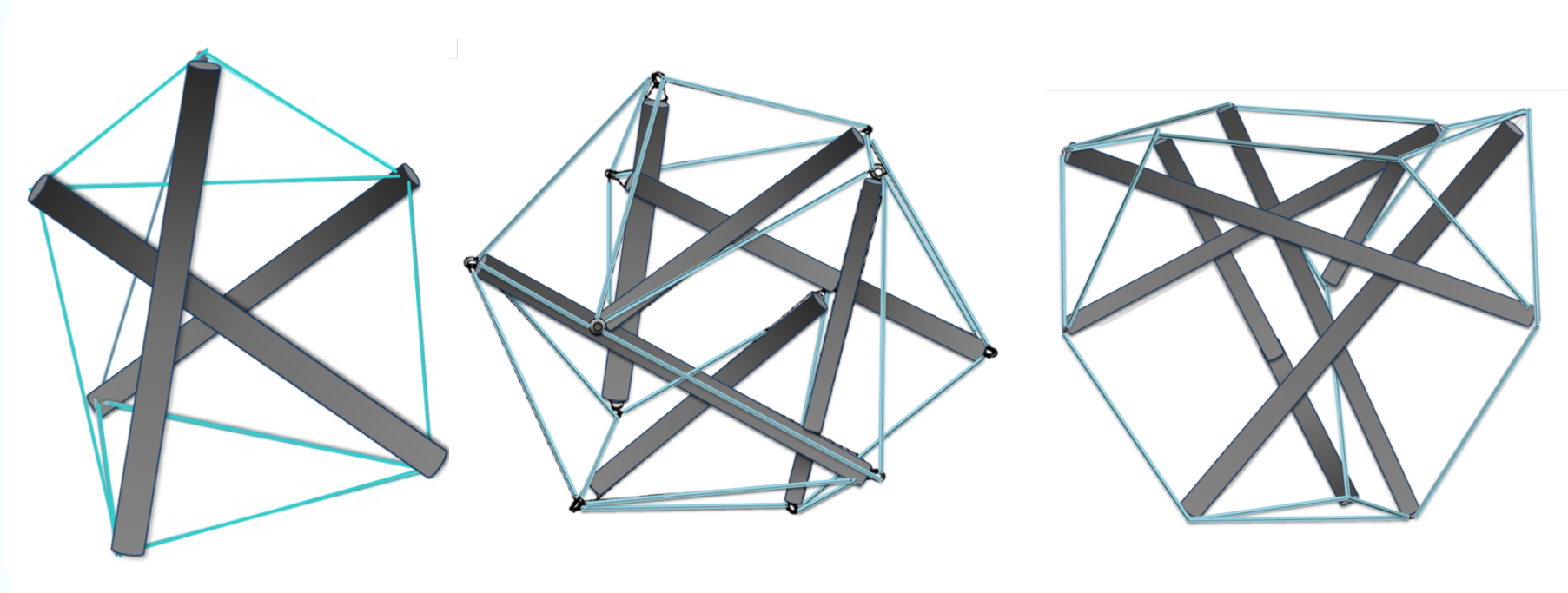


animation >



Motion (left) and contact force (right) animations for a 2D granular system transversally impacted by an external striker.

Tensegrity metamaterials

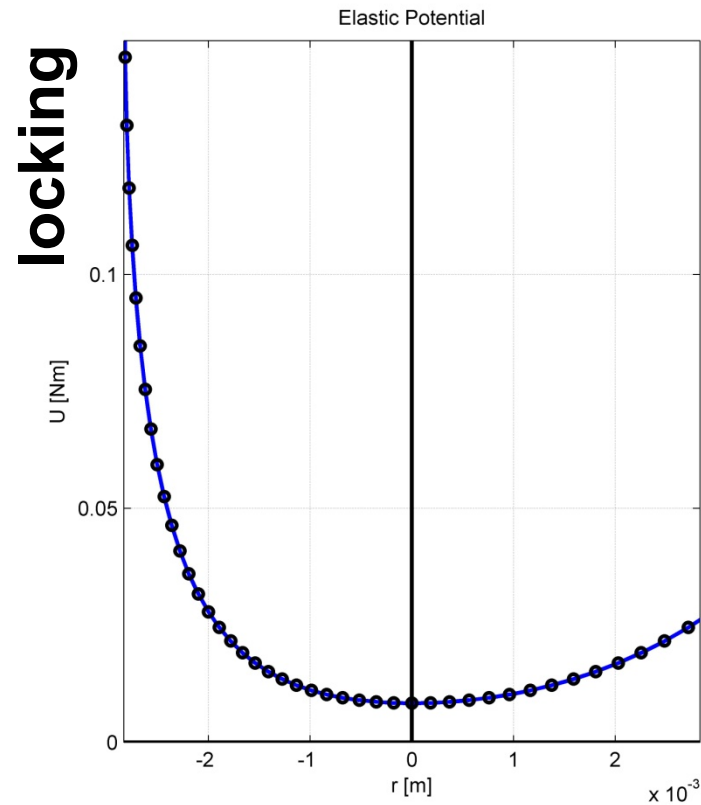
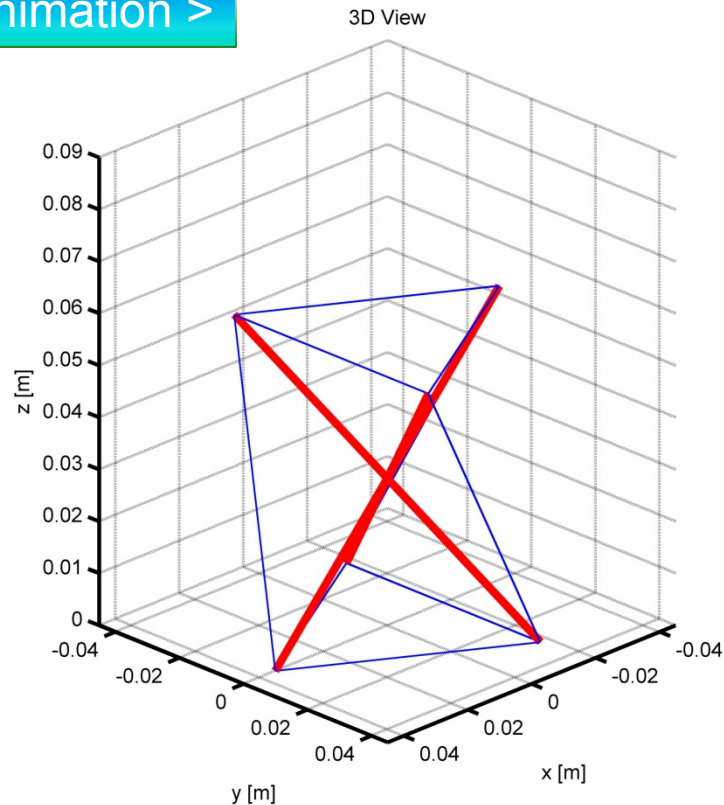


Tensegrity metamaterials are here defined as periodic arrays of tensegrity structures, freestanding or embedded in a matrix.

Such structures may act as "engineered structural foams" featuring special dynamics, due to the geometrically nonlinear response of the tensegrity units. The mechanical properties of the t-units can be adjusted on the fly, through suitable control of prestress and geometry of strings and bars.

Elastic potential of a hardening prism

animation >



It has been shown that tensegrity prisms endowed with rigid bases (“hard t-prisms”) feature a ‘locking’ behavior in compression. Such a behavior is characteristic of lattices supporting solitary waves featuring atomic-scale localization in the high-energy limit (Fraternali et al., 2012).

Control and deployability



Courtesy of Bob Skelton, UCSD

Part I

Basic Properties of Solitary Waves

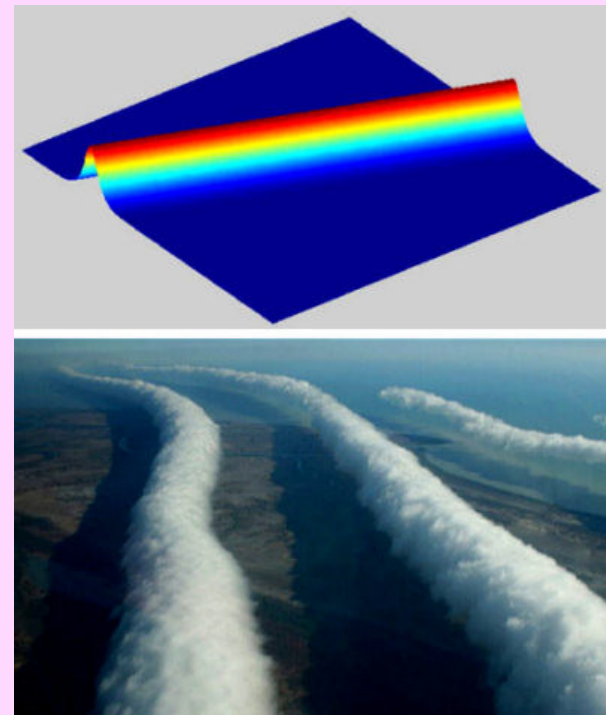
Solitons

A soliton (or solitary wave) is a solution of a nonlinear wave equation that asymptotically preserves the same shape and velocity after a collision with other solitary waves.

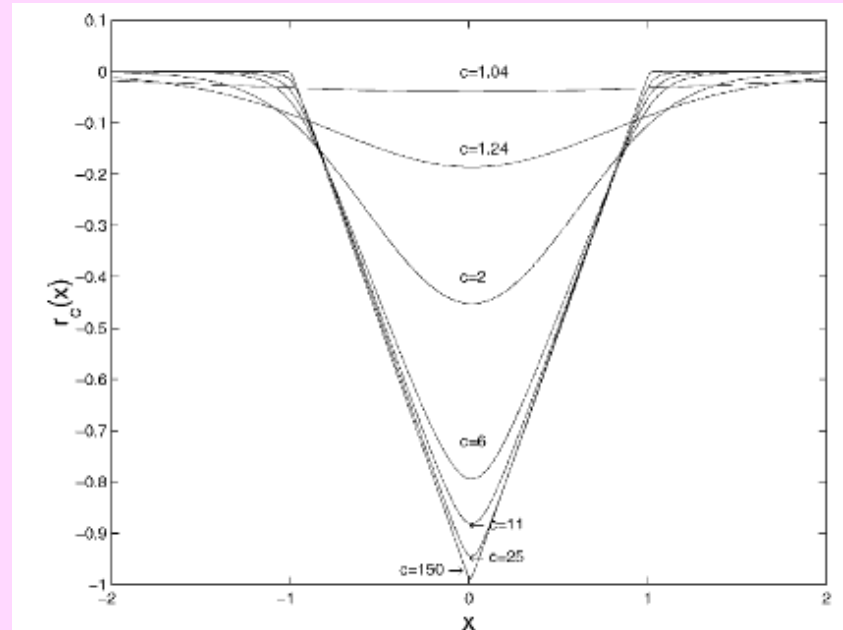
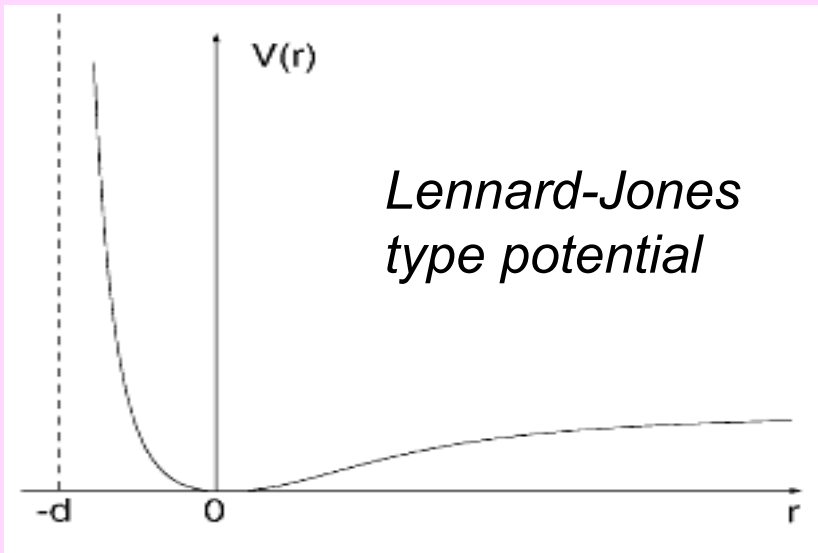
Properties:

- describe waves with permanent form;
- are localized, so that decay or approximate a constant to infinity;
- can interact strongly with other solitons, but emerge from the collisions unchanged unless a motion phase.

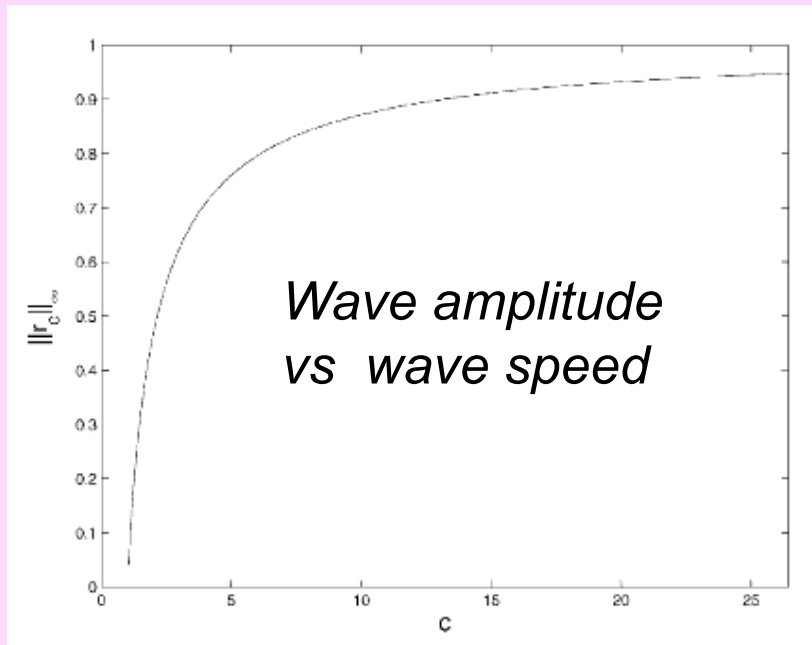
[animation >](#)



Super-compact solitary waves on stiffening lattices



Displacement wave profile

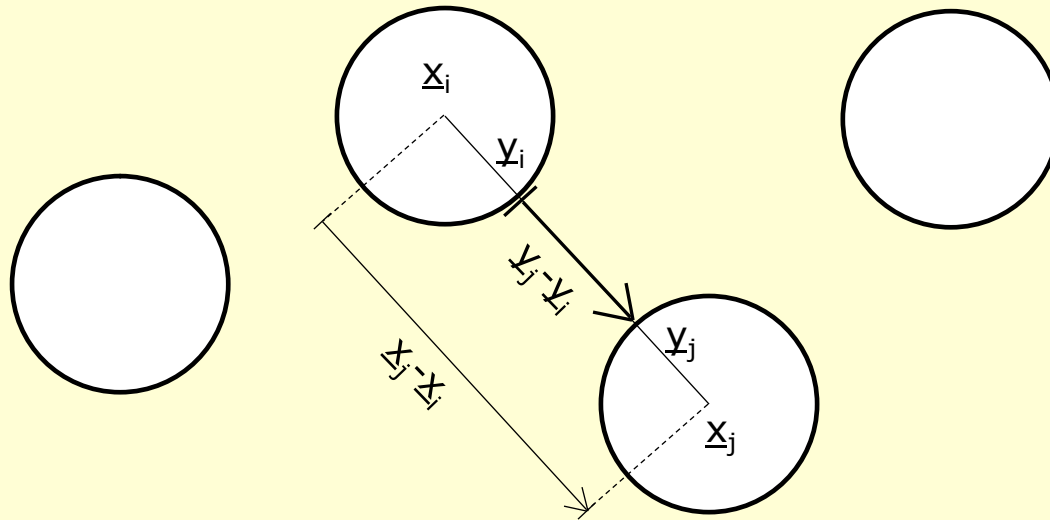


From Friesecke and Matthies, Physica D, 2002.

Part II

Optimal Design of Granular Protectors

Discrete element modeling



generalized coordinates

$$q_1, \dots, q_M$$

$$\underline{x}_i = \underline{x}_i(q_m)$$

position
vectors

$$\underline{y}_i = \underline{y}_i(q_m)$$

particle strains

(+ dilatation, - compression)

$$\delta_{ij} = (\underline{y}_j - \underline{y}_i) \cdot \frac{(\underline{x}_j - \underline{x}_i)}{|\underline{x}_j - \underline{x}_i|}$$

We employ a discrete element modeling of a granular metamaterial by describing the particles as point masses connected by nonlinear springs, which reproduce the Hertzian contact law between spheres.

Interaction potentials

Potential of the external forces

(gravity, precompression, etc.)

$$V = \sum_{i=1}^N \sum_{j>i} V_{ij}(\delta_{ij}(q_m)) - \sum_{i=1}^N W_i(q_m) \quad \text{Potential energy}$$

Hertz interaction potentials

$$V_{ij} = \frac{1}{n_{ij} + 1} \alpha_{ij} (\delta_{ij}^-)^{n_{ij} + 1} \quad \text{Interaction potentials}$$

$$F_{ij} = V'_{ij} = \alpha_{ij} (\delta_{ij}^-)^{n_{ij}} \quad \text{Interaction forces}$$

$$\delta_{ij}^- = \min\{0, \delta_{ij}\} \quad \text{Negative (compressive) part of } \delta_{ij} \\ \text{(no tension behavior)}$$

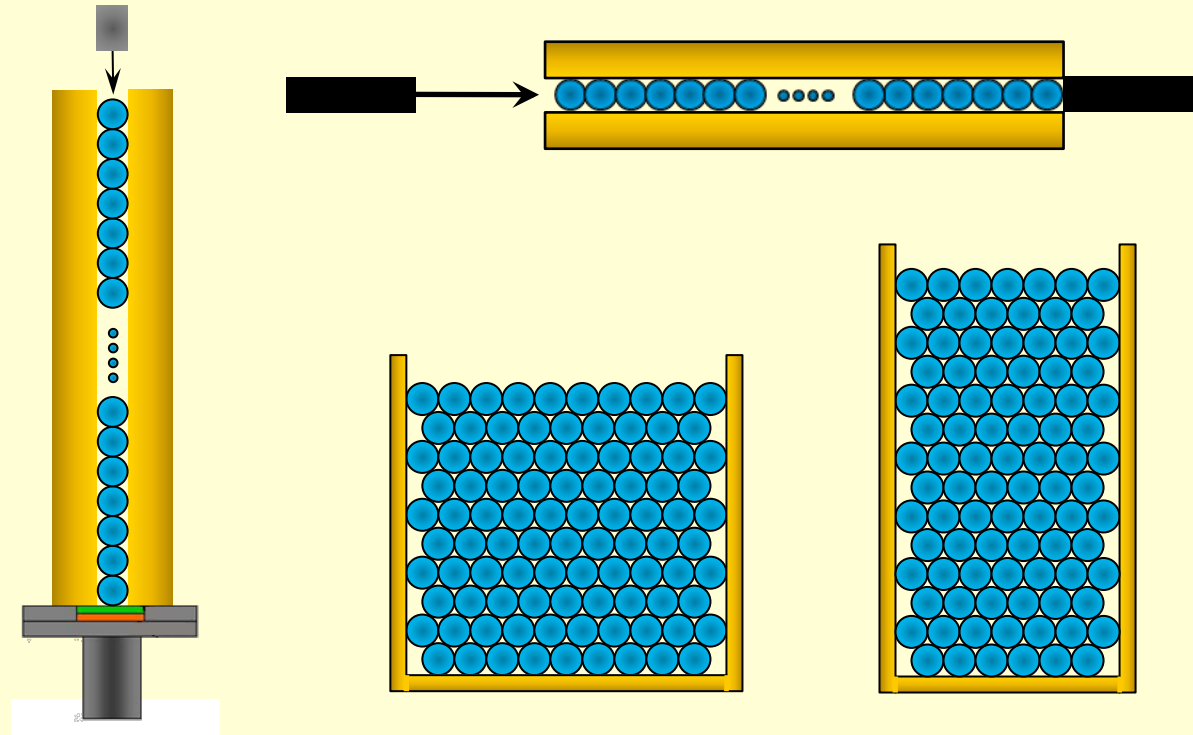
For spherical particles

$$\alpha_{ij} = \frac{4E_i E_j}{3E_j(1 - \nu_i^2) + 3E_i(1 - \nu_j^2)} \sqrt{\frac{r_i r_j}{r_i + r_j}}$$

$$n_{ij} = 1.5$$

Numerical results: optimization of 1D and 2D granular protectors

Analyzed systems and materials



- Steel beads
- PTFE beads
- Rubber beads
- Bronze beads
- Glass beads
- Nylon beads

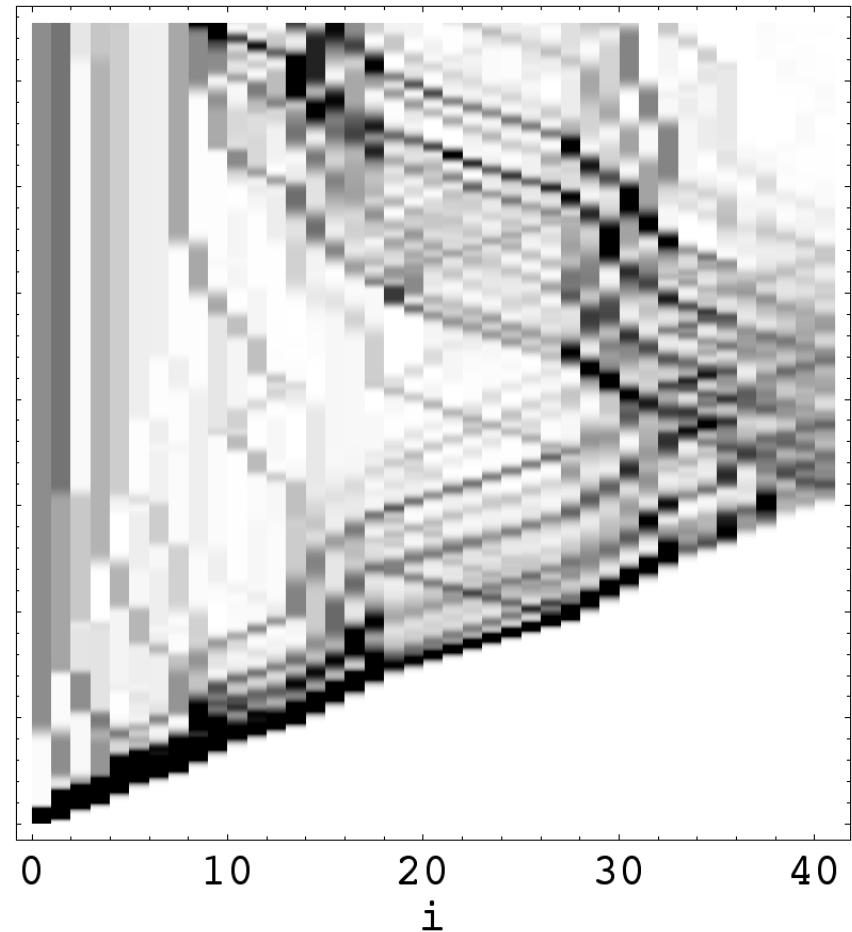
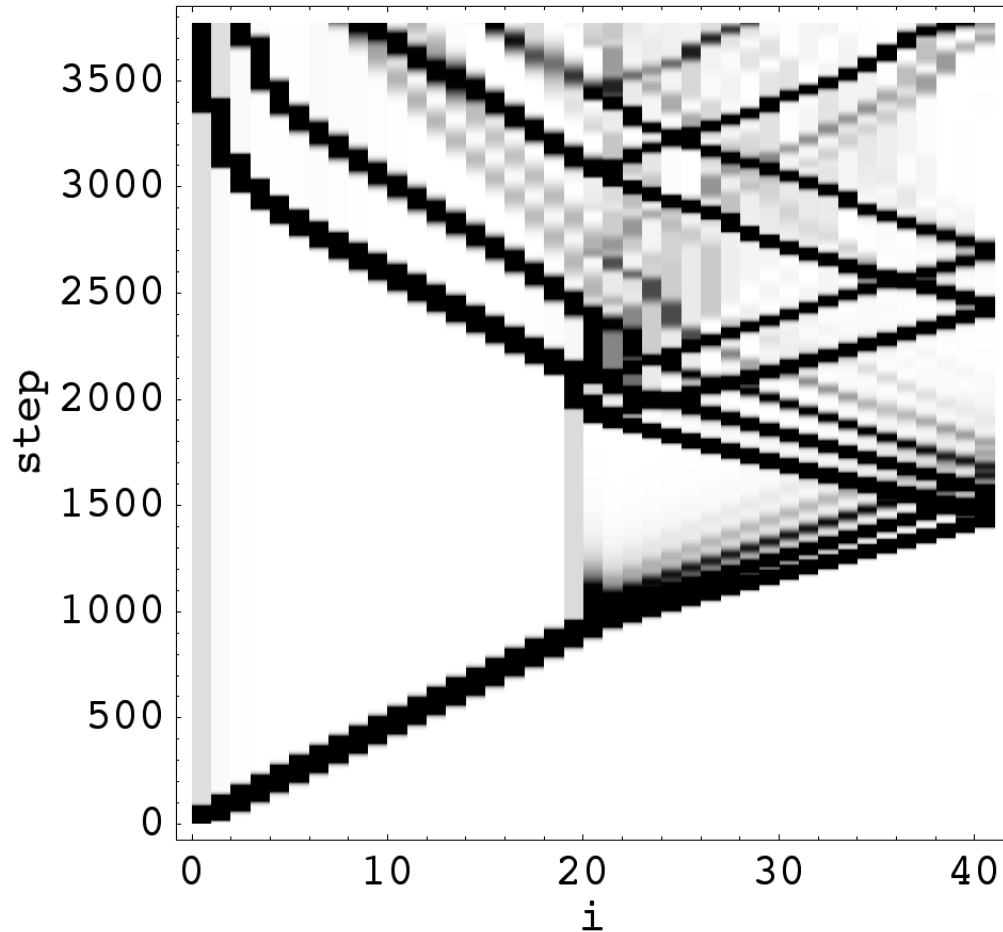
	Elastic modulus [GPa]	Poisson's ratio	Density [kg/m ³]
Stainless steel	193,00	0,30	8000
PTFE	1,46	0,46	2200
Rubber	0,30	0,49	2200
Bronze	76,00	0,41	8500
Glass	62,00	0,20	2425
Nylon	3,55	0,40	1085

Topology optimization

Stepped 2SV

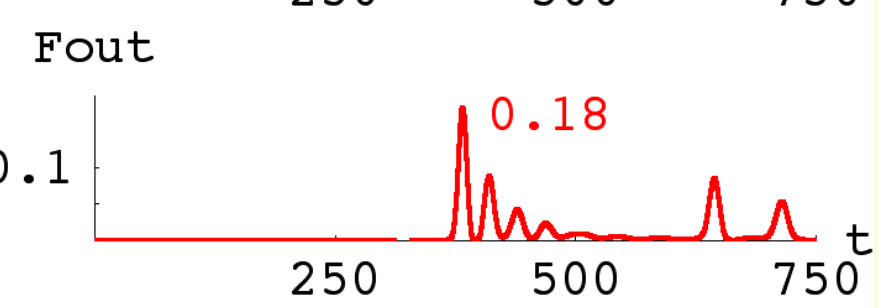
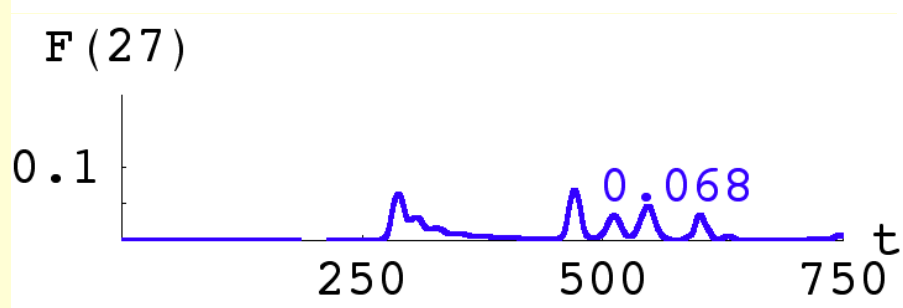
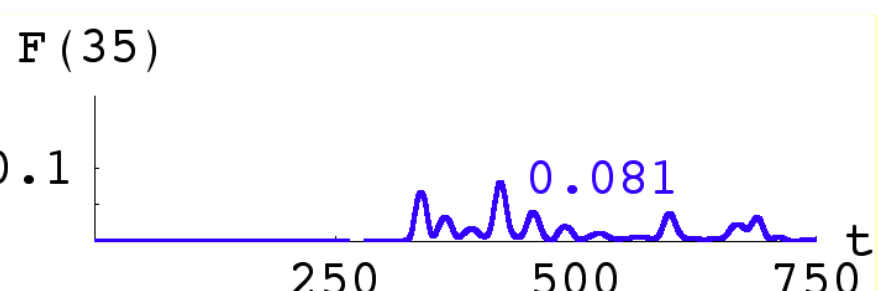
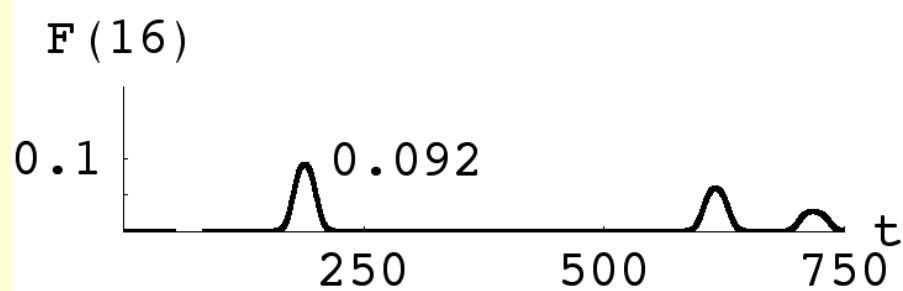
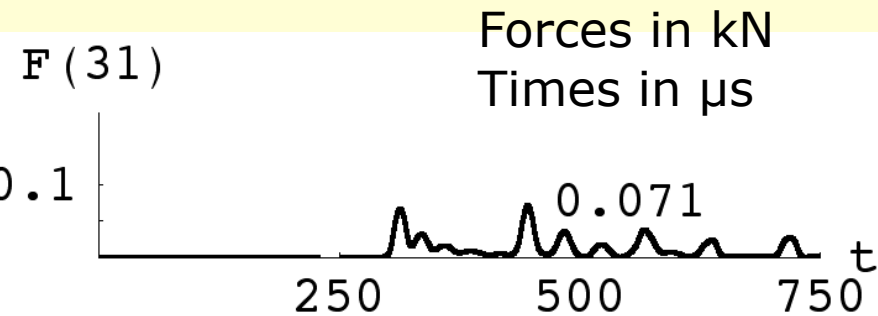
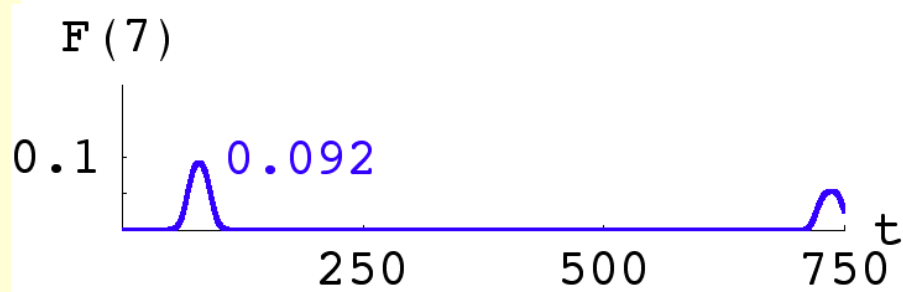
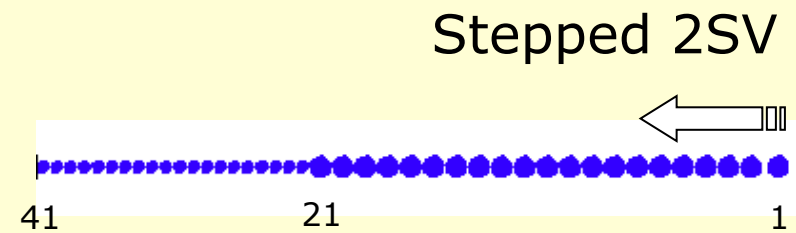
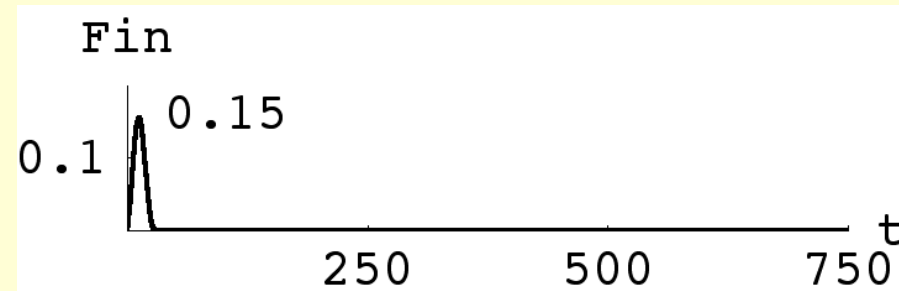


Optimized system

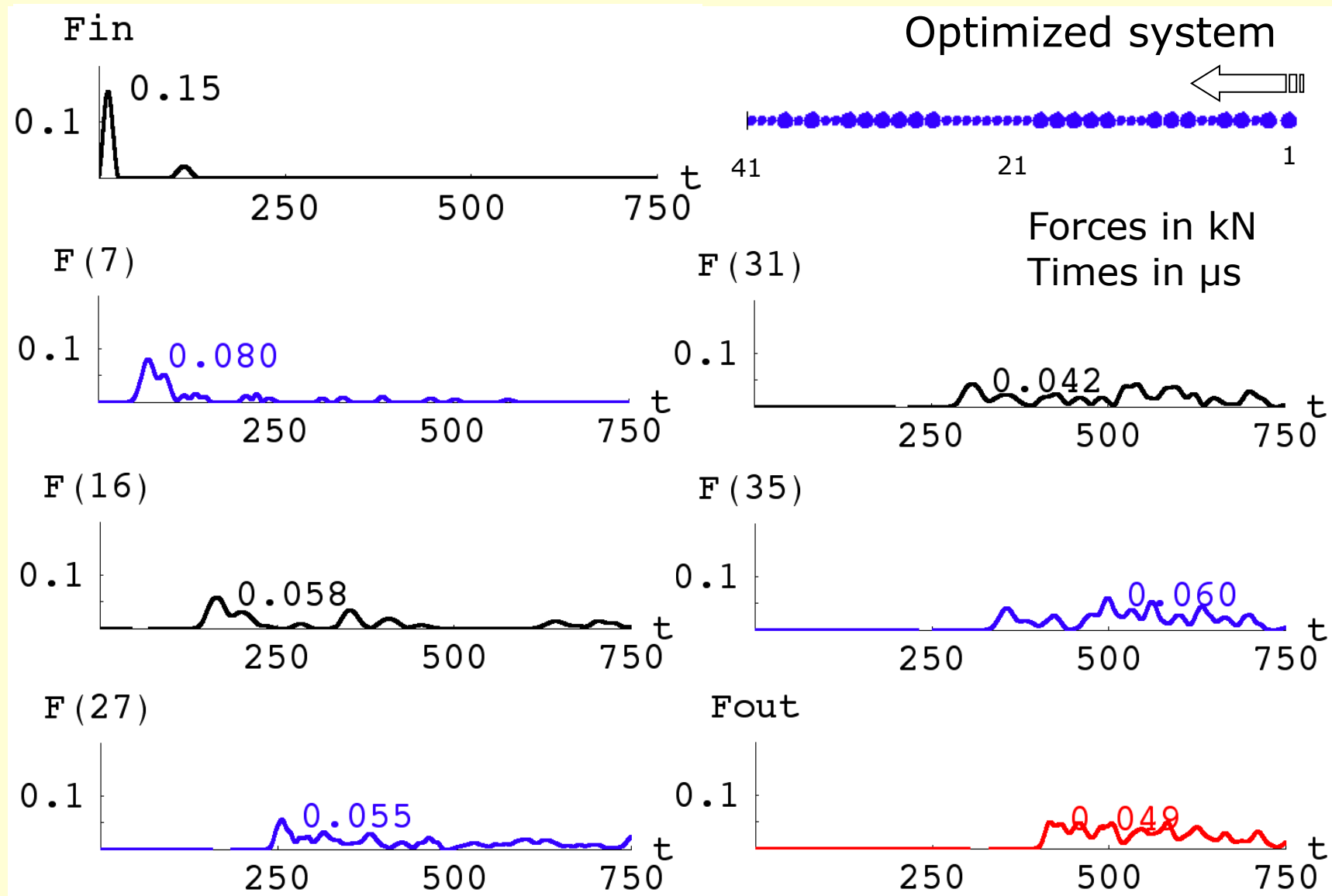


Density plots of particle energies normalized to unity.

Topology optimization

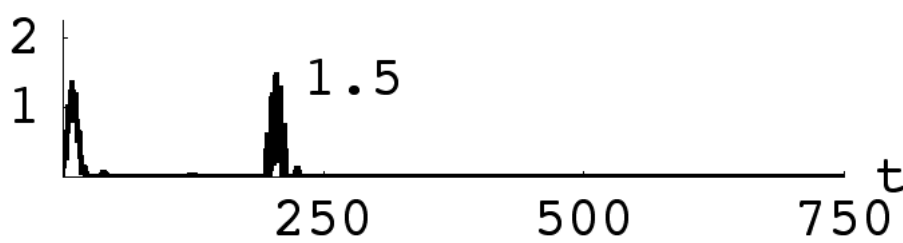


Topology optimization

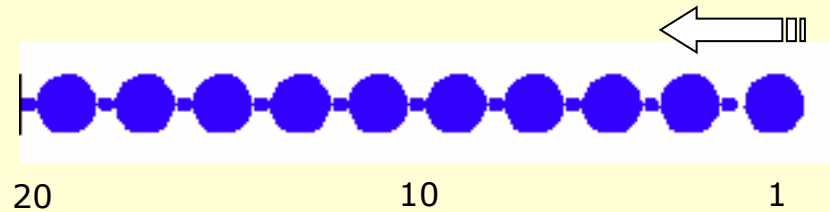


Size optimization

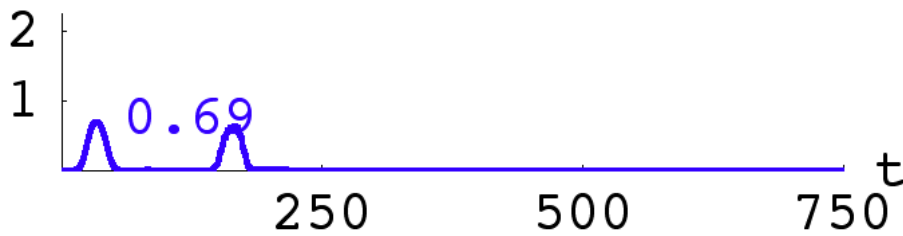
Fin



"Decorated" chain

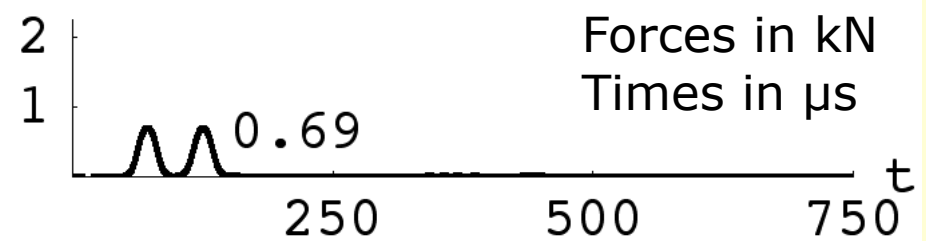


F (7)

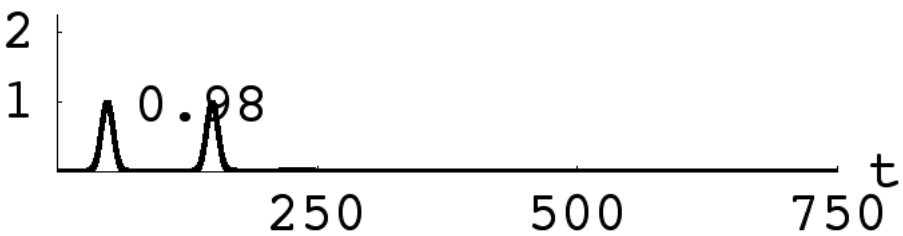


F (15)

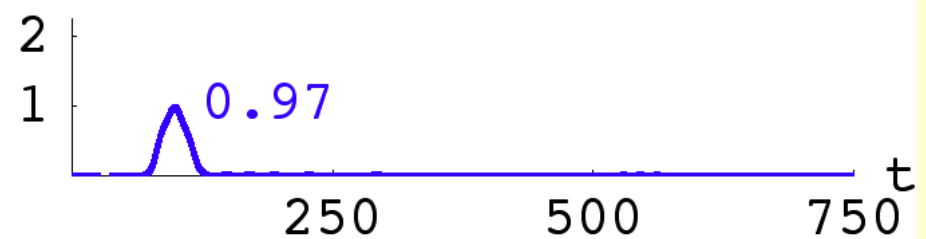
$v(1)_{t=0} = 18.88 \text{ m/s}$



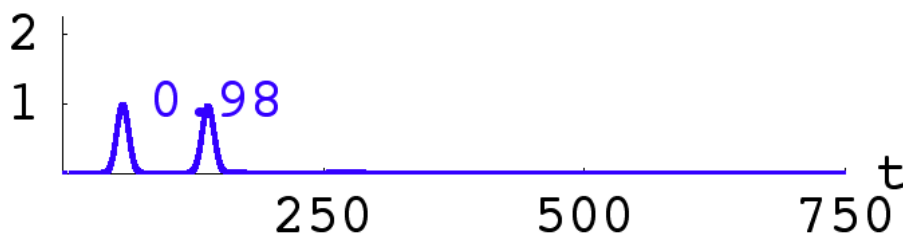
F (10)



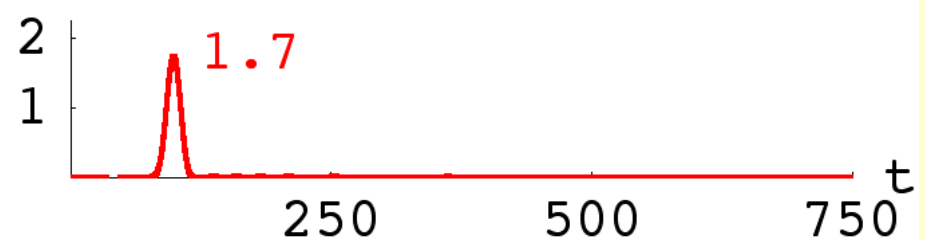
F (19)



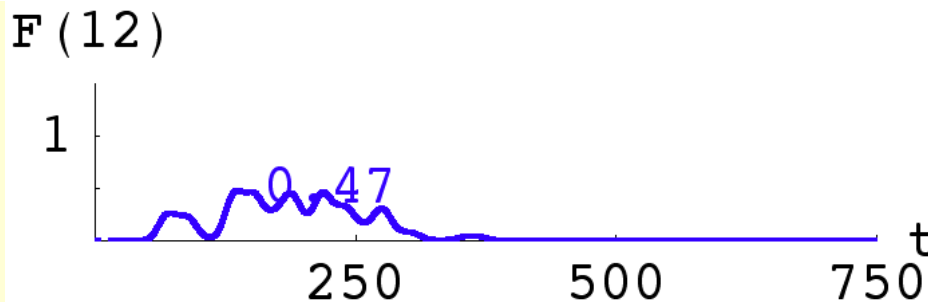
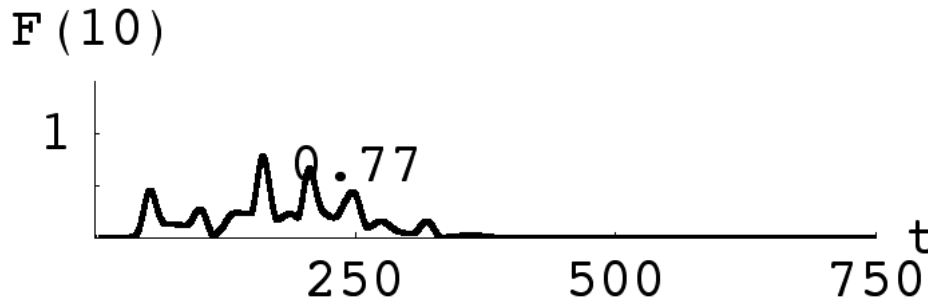
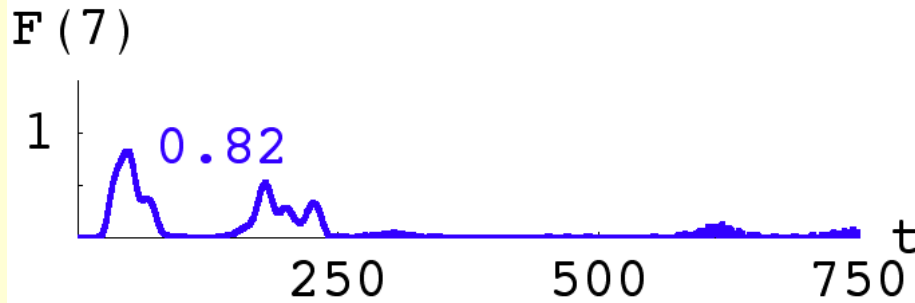
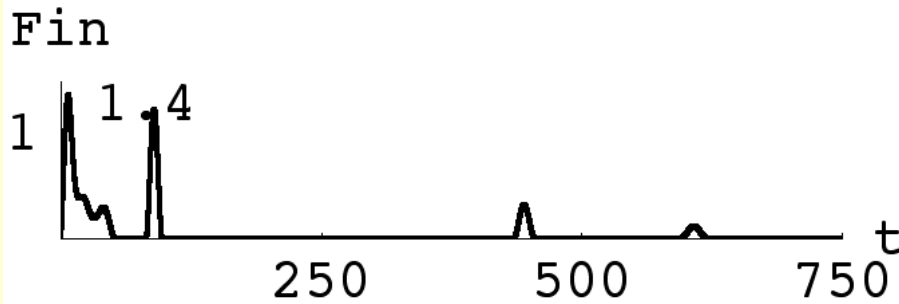
F (12)



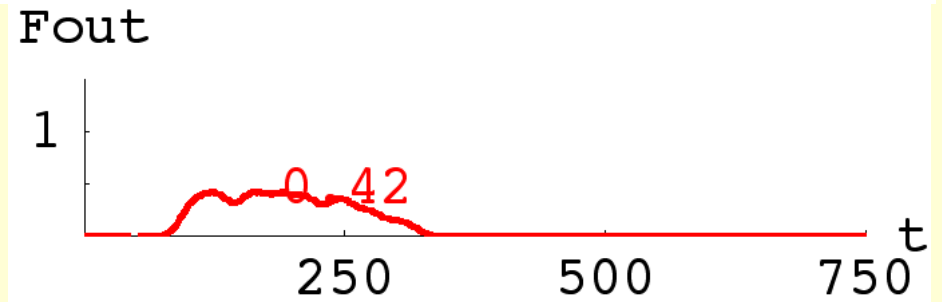
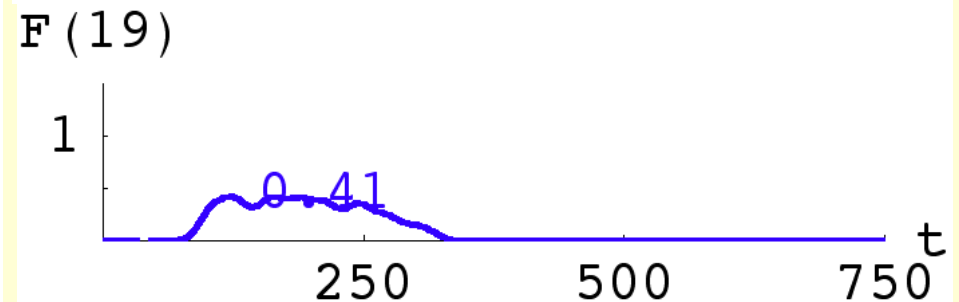
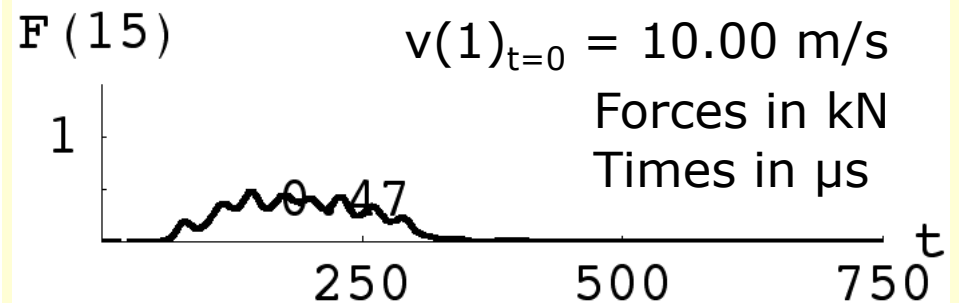
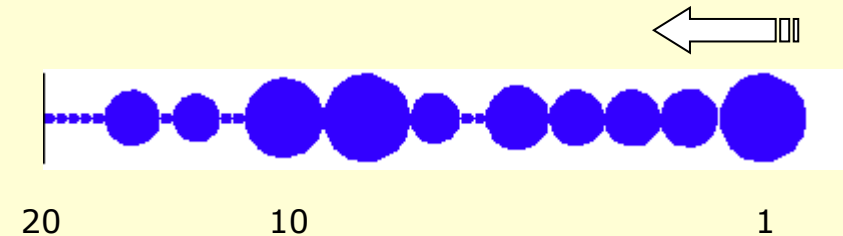
Fout



Size optimization

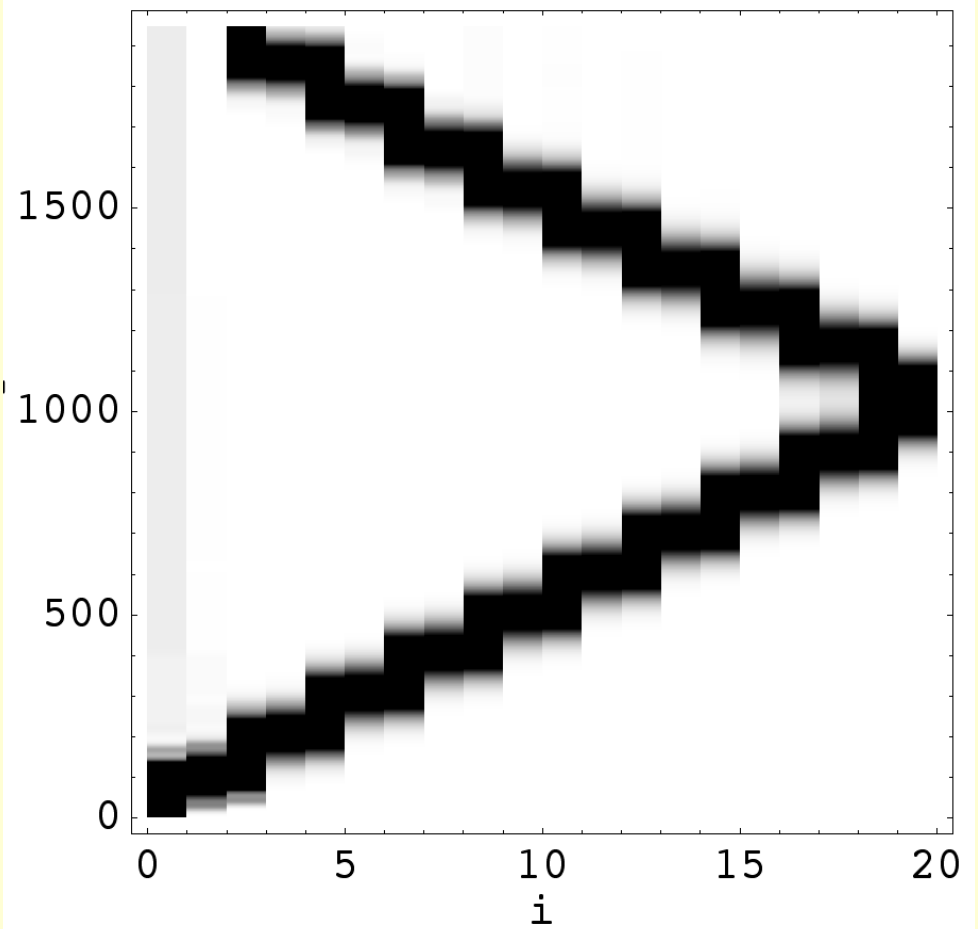


Optimized system

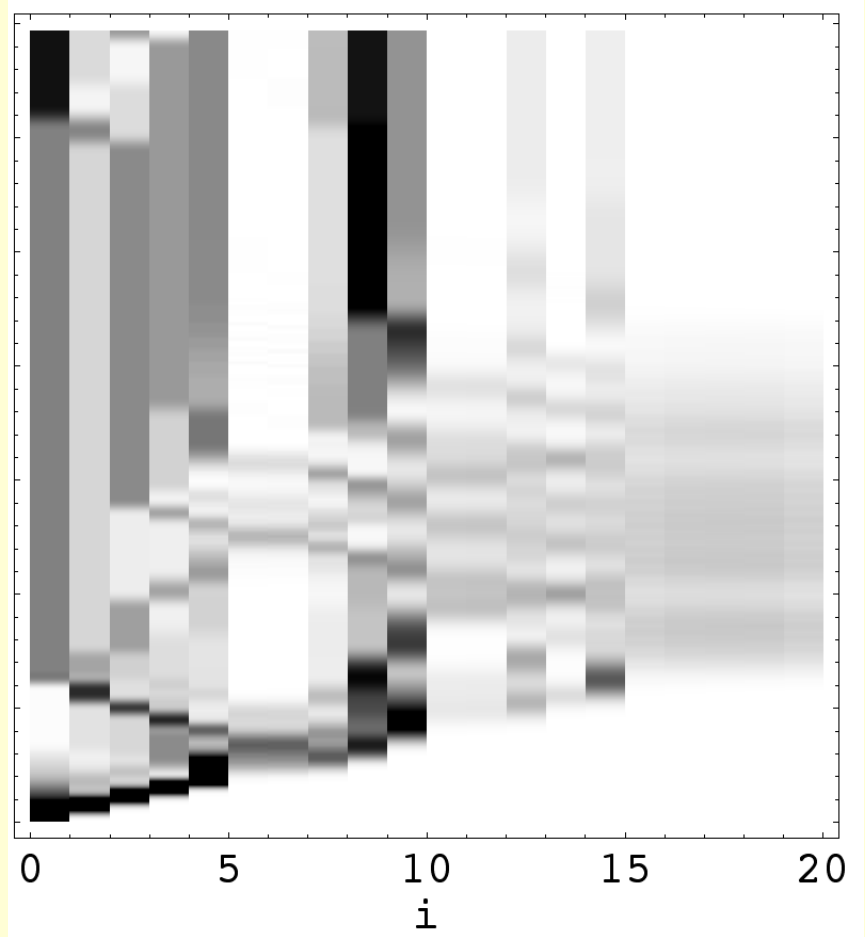


Size optimization

“Decorated” chain

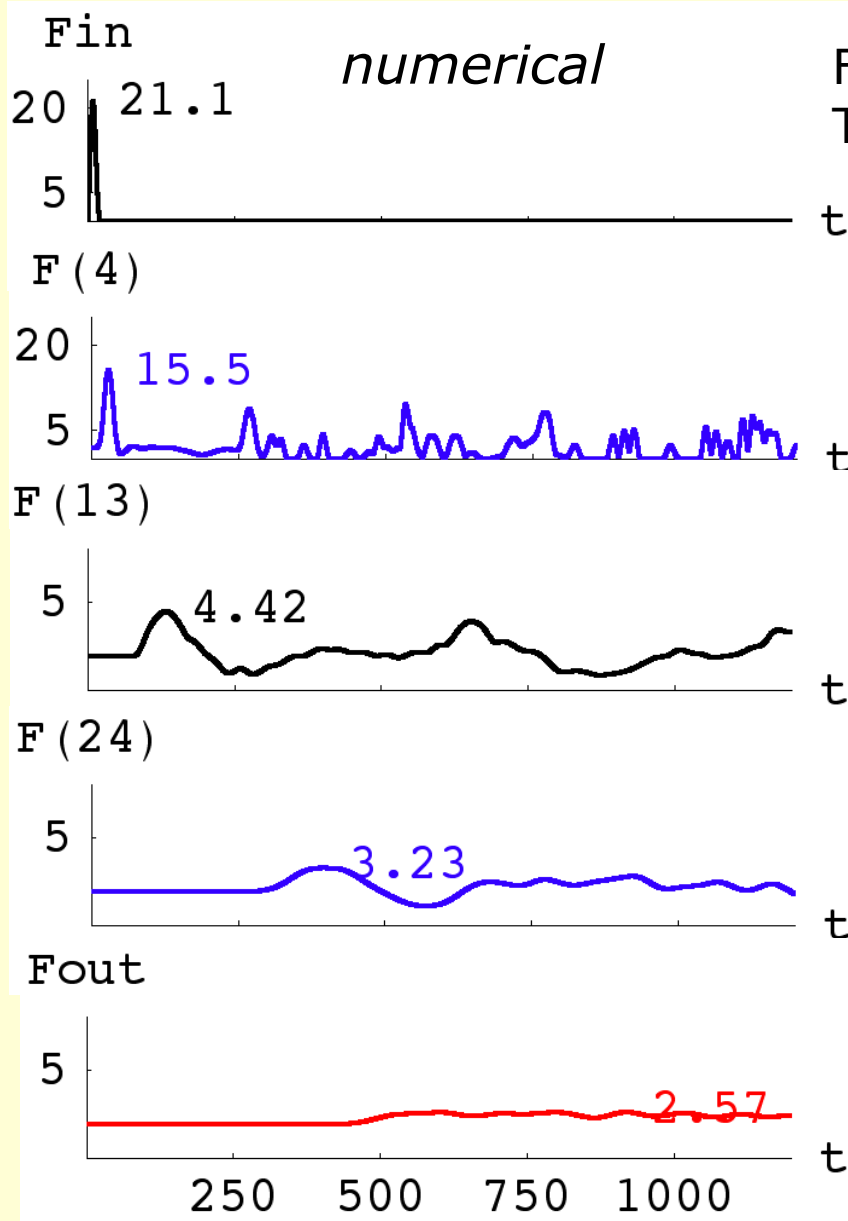


Optimized system



Density plots of particle energies normalized to unity.

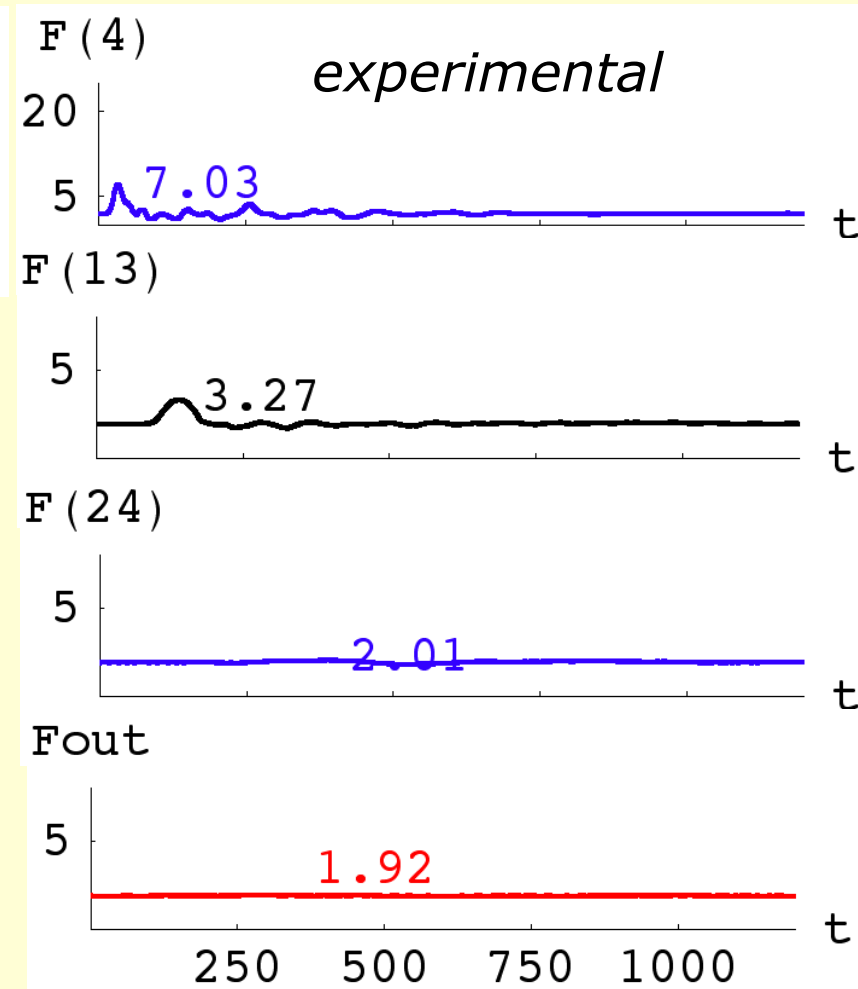
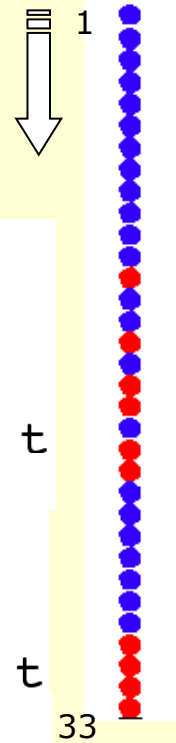
Material optimization



Forces in N
Times in μs

Optimized system

- steel
- ptfе

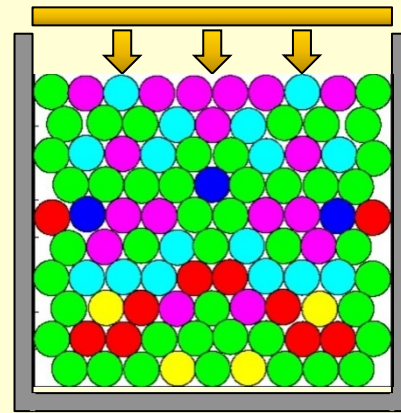


2D granular crystals/systems

composite
10x0 box-
uniform impact

$F_{out} = 159 \text{ N}$

[animation >](#)

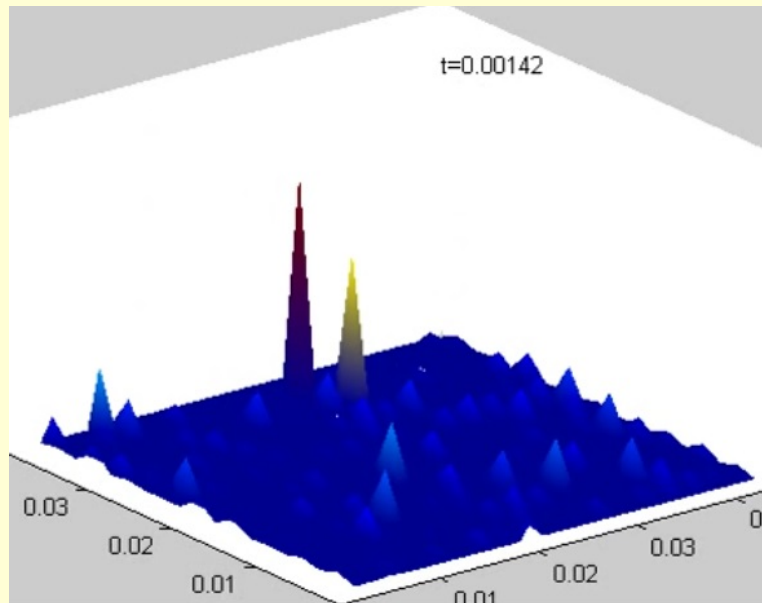
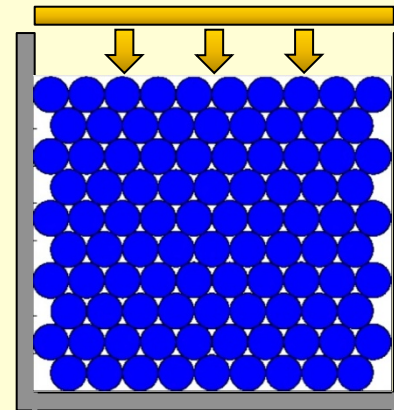


$v = 10 \text{ m/s}$

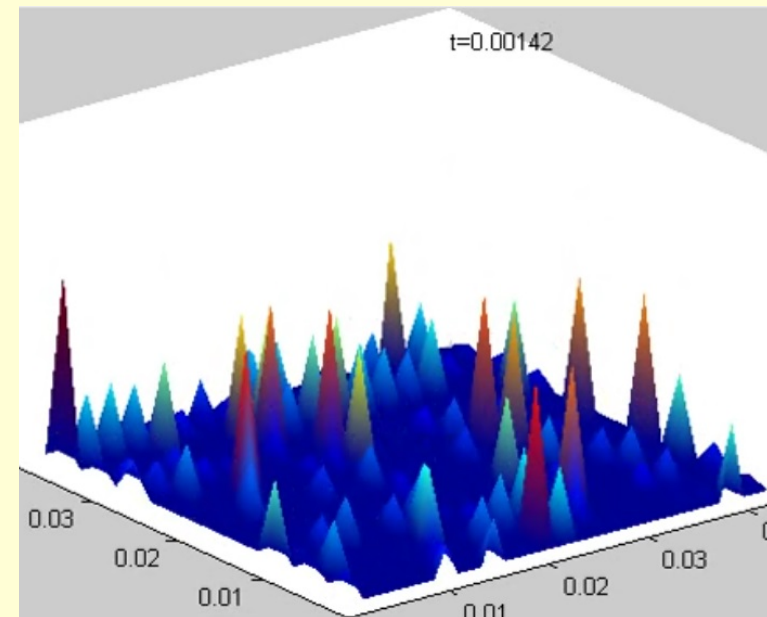
homogeneous
10x0 steel box-
uniform impact

$F_{out} = 2011 \text{ N}$

[animation >](#)



[animation >](#)



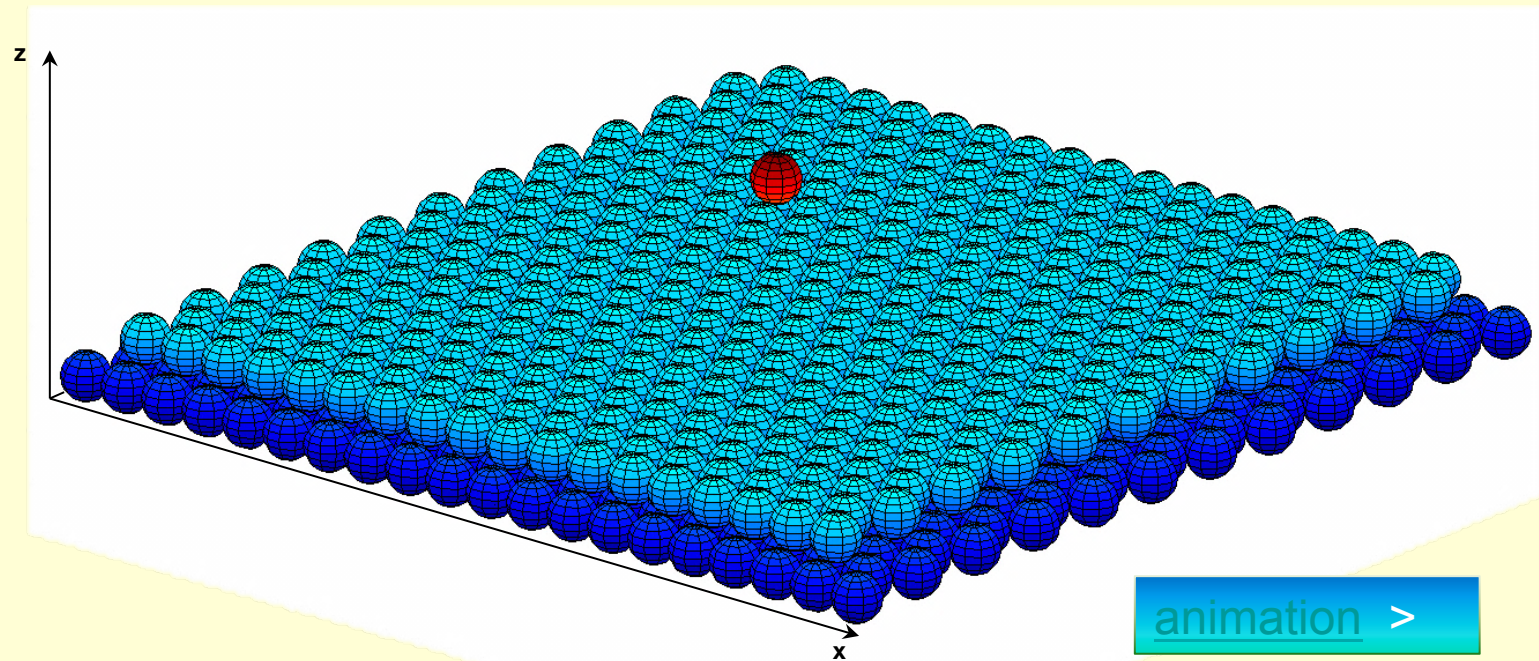
[animation >](#)

Contact forces

3D granular crystals/systems

no. of beads= 833
diameter= 9.53 mm

v striker = 1.65 m/s
material: stainless steel



***Force mitigation efficiency
at the lateral walls: 95%***

***Force mitigation efficiency at
the bottom wall: 70%***

Discussion

We have show that an optimized design may lead to dramatic advantages in the protection abilityof granular protectors, leading to a significant decrease of the transmitted force.

In particular, an optimal design may generate suitable topology, size, and material randomization by combining effects of wave disintegration and reflection at the interfaces between different particles.

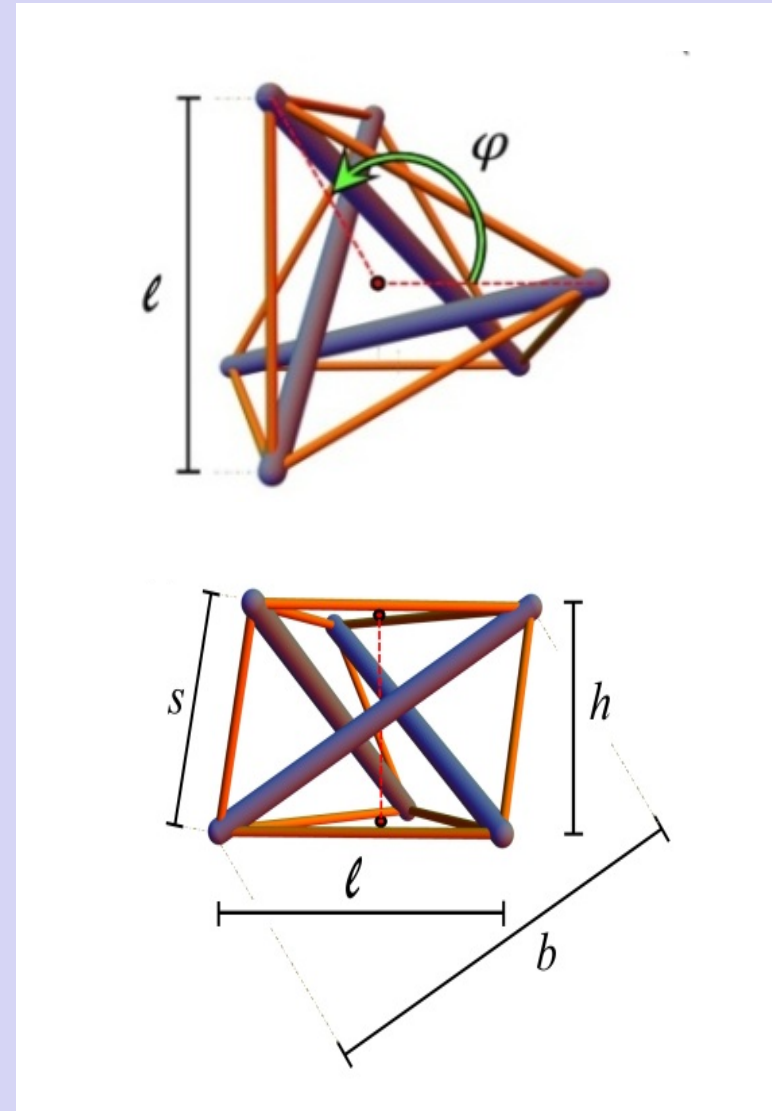
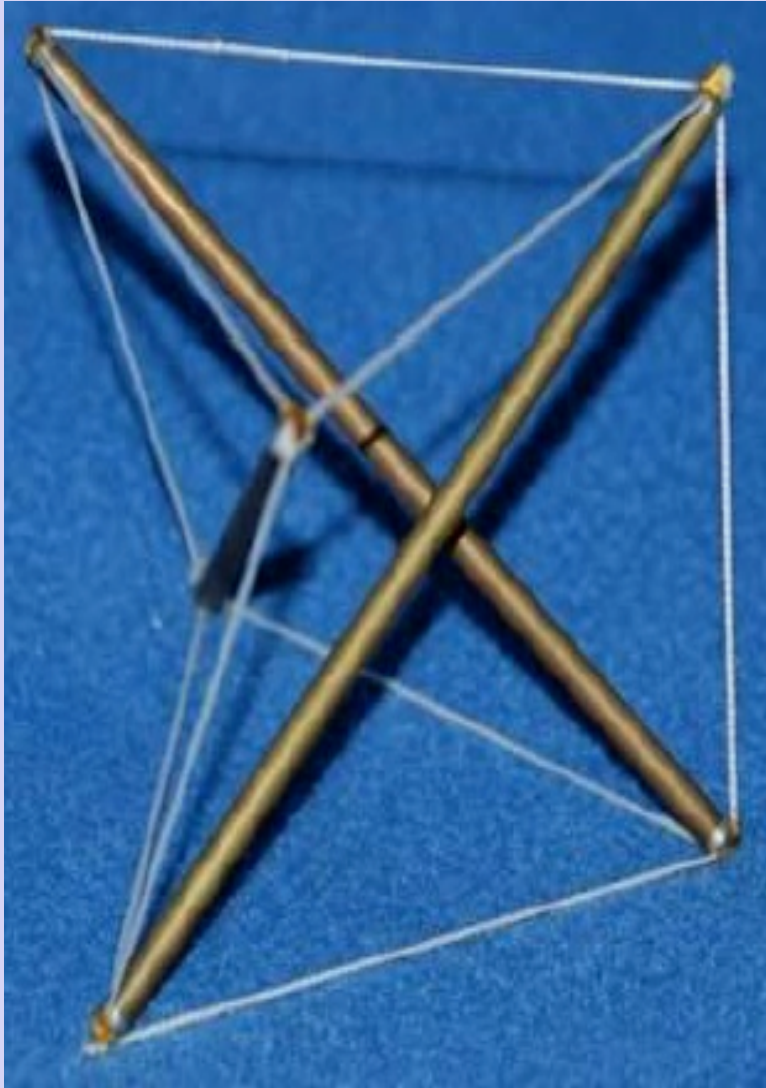
A general feature we observe in the optimized protectors is the transformation of incident waves into a collection of interacting reflected and transmitted solitary pulses, which in particular form an extended (long-wavelength), small-amplitude wave that travels to the wall.

We also find that optimization randomizes these systems (adding to their disorder) and produces a marked thermalization. We constantly observe the appearance of soft/light beads near the wall, hard/heavy beads near the end impacted by the striker, and alternating hard and soft beads in the central section of the optimized protectors.

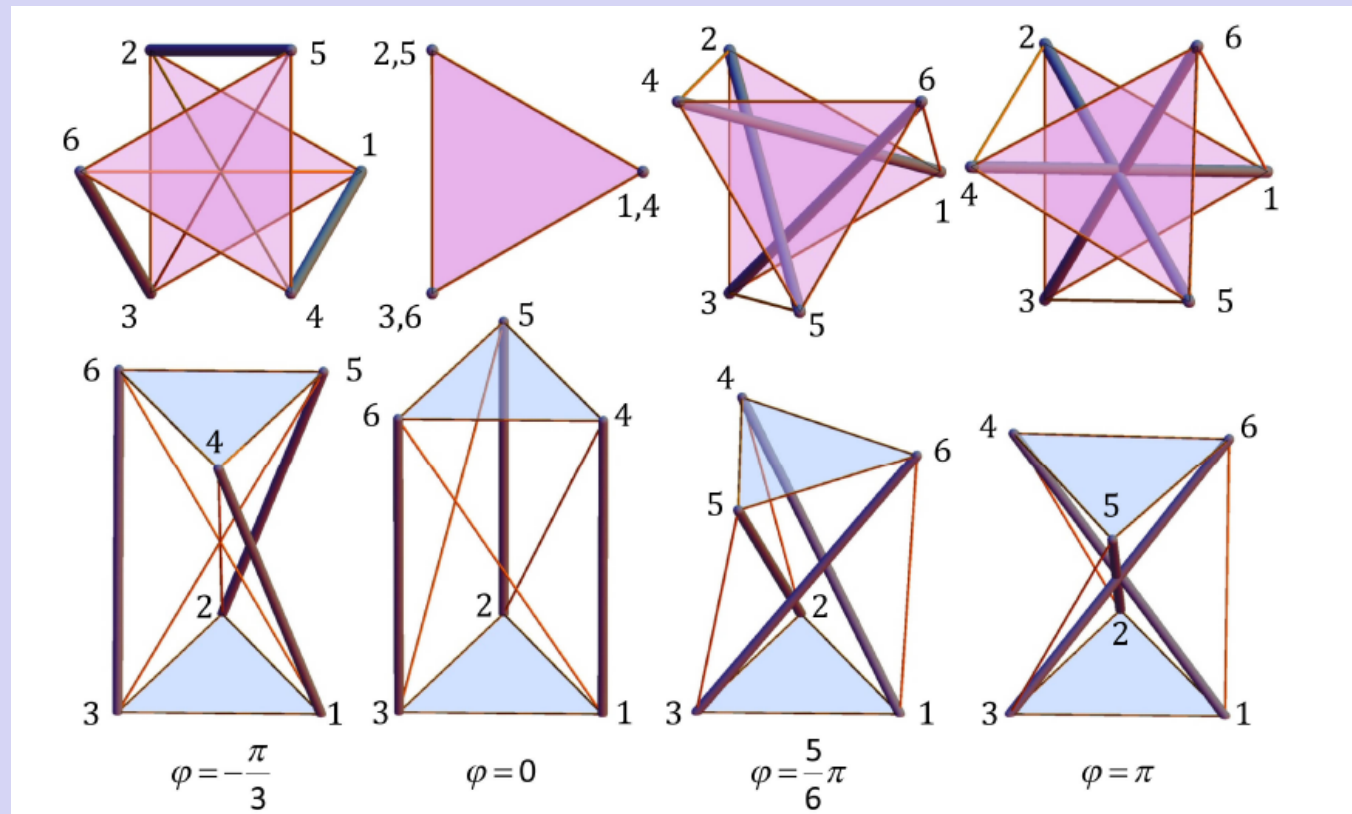
Part III

Solitary Waves on Tensegrity Metamaterials

Mechanical response of a tensegrity prism under axial loading



Sequence of configurations corresponding to feasible values of the twisting angle



Compatibility equations

$$b = \sqrt{h^2 - \frac{2}{3}\ell^2 \cos(\varphi) + \frac{2\ell^2}{3}}, \quad \left(h = \sqrt{b^2 - \frac{2}{3}\ell^2(1 - \cos \varphi)} \right),$$

$$s = \frac{\sqrt{3h^2 - \sqrt{3}\ell^2 \sin(\varphi) + \ell^2 \cos(\varphi) + 2\ell^2}}{\sqrt{3}}$$

Equilibrium problem

$$\begin{aligned}x_1 &= -\frac{2F \sin(\varphi)}{3\sqrt{3}h (\sqrt{3} \sin(\varphi) + \cos(\varphi))} \\x_2 &= -\frac{F (\sin^2(\varphi) - \sqrt{3} \sin(\varphi) + \cos^2(\varphi) - \cos(\varphi))}{9h (\sqrt{3} \sin(\varphi) + \cos(\varphi))} \\x_3 &= \frac{F}{3h} - \frac{2F \sin(\varphi)}{3\sqrt{3}h (\sqrt{3} \sin(\varphi) + \cos(\varphi))}\end{aligned}$$

General solution to nodal equilibrium equations (x_1 , x_2 , x_3 : force densities in cross-strings, base-strings and bars, respectively)

$$\varphi = -\frac{\pi}{6} : x_2 = -\frac{x_1}{\sqrt{3}}, \quad x_3 = x_1$$

$$\varphi = \frac{5}{6}\pi : x_2 = \frac{x_1}{\sqrt{3}}, \quad x_3 = x_1$$

5

Prestressable configurations

Elastic problem $\left(x_1 = \frac{k_1(s-s_N)}{s}, x_2 = \frac{k_2(\ell-\ell_N)}{\ell}, x_3 = \frac{k_3(b-b_N)}{b} \right)$

$$g_1 = \frac{1}{6}\ell \left(k_3 4 \sin^2\left(\frac{\varphi}{2}\right) \left(\sqrt{3} - \frac{3b_N}{\sqrt{3h^2 - 2\ell^2 \cos(\varphi) + 2\ell^2}} \right) \right. \\ \left. + k_1 \left(-3 \sin(\varphi) + \sqrt{3} \cos(\varphi) + 2\sqrt{3} \right) + k_2 \frac{6\sqrt{3}(\ell - \ell_N)}{\ell} \right. \\ \left. - k_1 \frac{3s_N \left(-\sqrt{3} \sin(\varphi) + \cos(\varphi) + 2 \right)}{\sqrt{3h^2 - \sqrt{3}\ell^2 \sin(\varphi) + \ell^2 \cos(\varphi) + 2\ell^2}} \right) = 0$$

$$g_2 = \frac{1}{6}\ell \left(k_3 2 \sin(\varphi) \left(\frac{3b_N}{\sqrt{3h^2 - 2\ell^2 \cos(\varphi) + 2\ell^2}} - \sqrt{3} \right) \right. \\ \left. + k_1 \left(\sqrt{3} \sin(\varphi) + 3 \cos(\varphi) \right) \right. \\ \left. - k_1 \frac{3s_N \left(\sin(\varphi) + \sqrt{3} \cos(\varphi) \right)}{\sqrt{3h^2 - \sqrt{3}\ell^2 \sin(\varphi) + \ell^2 \cos(\varphi) + 2\ell^2}} \right) = 0$$

$$g_3 = -f + k_3 h \left(\frac{b_N}{\sqrt{h^2 - \frac{2}{3}\ell^2 \cos(\varphi) + \frac{2\ell^2}{3}}} - 1 \right) \\ + k_1 h \left(\frac{\sqrt{3}s_N}{\sqrt{3h^2 - \sqrt{3}\ell^2 \sin(\varphi) + \ell^2 \cos(\varphi) + 2\ell^2}} - 1 \right) = 0$$

Numerical approach

Continuation method

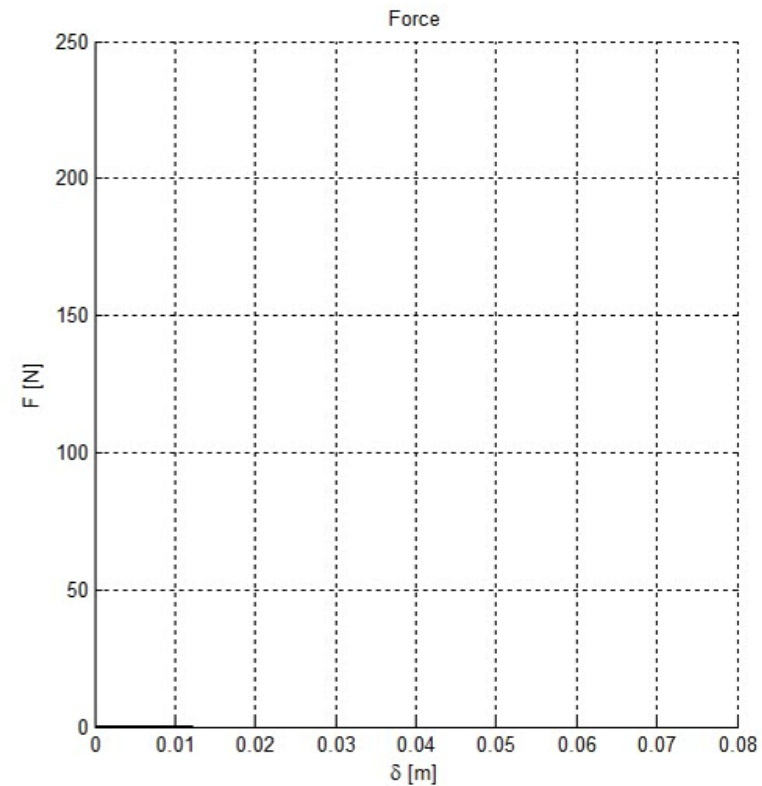
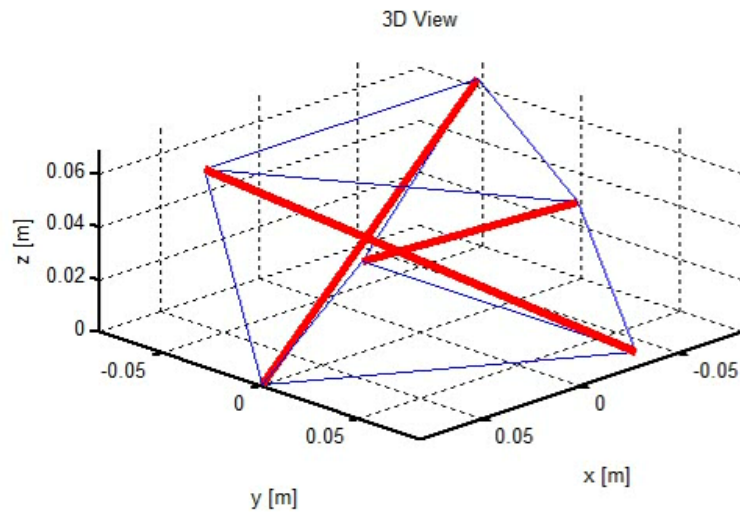
$$\mathbf{v} = [\ell, \varphi, h]^T, \quad \mathbf{g} = [g_1, g_2, g_3]^T,$$

$$\tilde{\mathbf{g}} = \begin{bmatrix} \mathbf{g}(\mathbf{v}, f) \\ \psi(\mathbf{v}, f) \end{bmatrix} = 0 \quad \begin{bmatrix} \nabla_{\mathbf{v}} \mathbf{g} & \nabla_f \mathbf{g} \\ \nabla_{\mathbf{v}} \psi^T & \nabla_f \psi \end{bmatrix} \begin{bmatrix} \Delta \mathbf{v} \\ \Delta f \end{bmatrix} = - \begin{bmatrix} \bar{\mathbf{g}} \\ \bar{\psi} \end{bmatrix}$$

Axial stiffness

$$K_{ho}^{el} = \frac{p_0}{1+p_0} \left\{ 36k_1\eta_0^2 \left((3+2\sqrt{3}+\sqrt{3}\eta_0^2)k_1k_2 + (-2+\sqrt{3}-\eta_0^2)k_1k_1 \frac{p_0}{1+p_0} \right. \right. \\ \left. \left. -6k_2k_1 \frac{p_0}{1+p_0} + k_3(2\sqrt{3}k_1 + (-3+2\sqrt{3}+\sqrt{3}\eta_0^2)k_2 - (2+\sqrt{3}+\eta_0^2) \right. \right. \\ \left. \left. \times k_1 \frac{p_0}{1+p_0} \right) \right\} / \left\{ 6k_1 \frac{p_0}{1+p_0} \left(\sqrt{3}(1+8\eta_0^2+2\eta_0^4)k_2 - 2\eta_0^4k_1 \frac{p_0}{1+p_0} \right) \right. \\ \left. + k_1 \left(3(2+\sqrt{3}+\eta_0^2)k_2 + (-3+2\sqrt{3}+(-24+13\sqrt{3})\eta_0^2)k_1 \frac{p_0}{1+p_0} \right) \right. \\ \left. + k_3 \left(6k_1 + 3(2-\sqrt{3}+\eta_0^2)k_2 + (3+2\sqrt{3}+(24+13\sqrt{3})\eta_0^2)k_1 \frac{p_0}{1+p_0} \right) \right\}$$

Force-displacement response of a fully-elastic prism



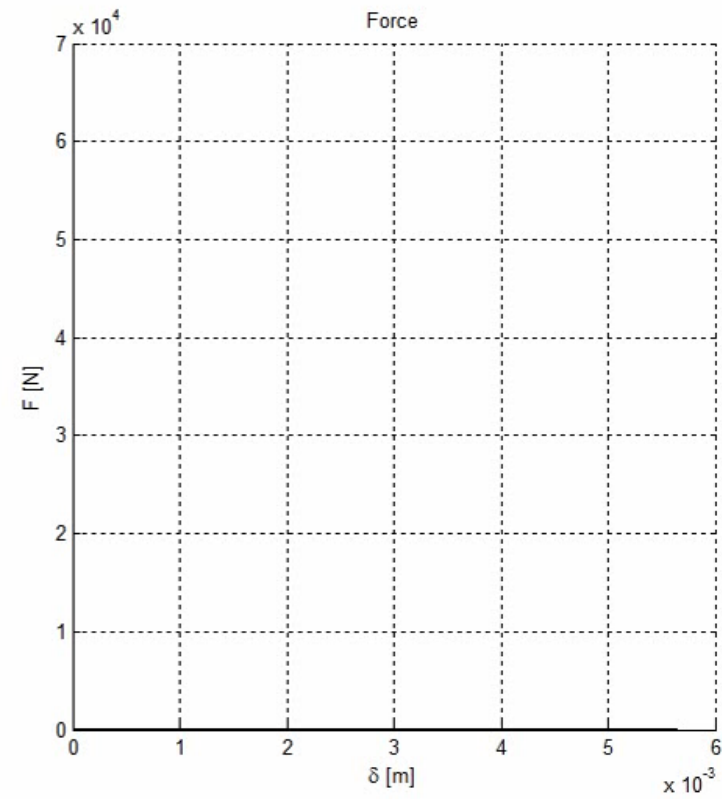
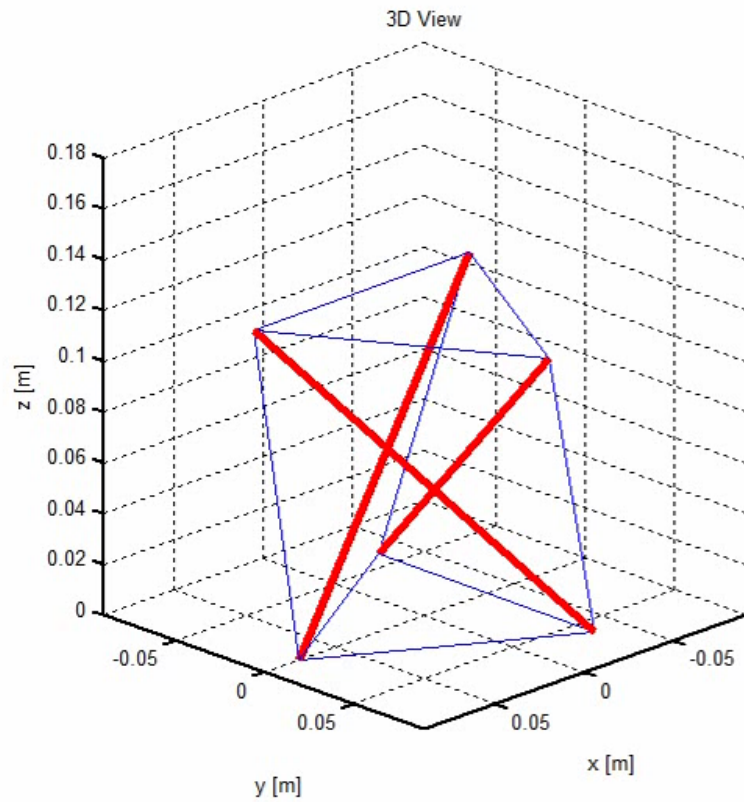
$$h = \sqrt{b^2 - \frac{2}{3}\ell^2(1 - \cos \varphi)}$$

Rigid-elastic model (ℓ and b fixed)

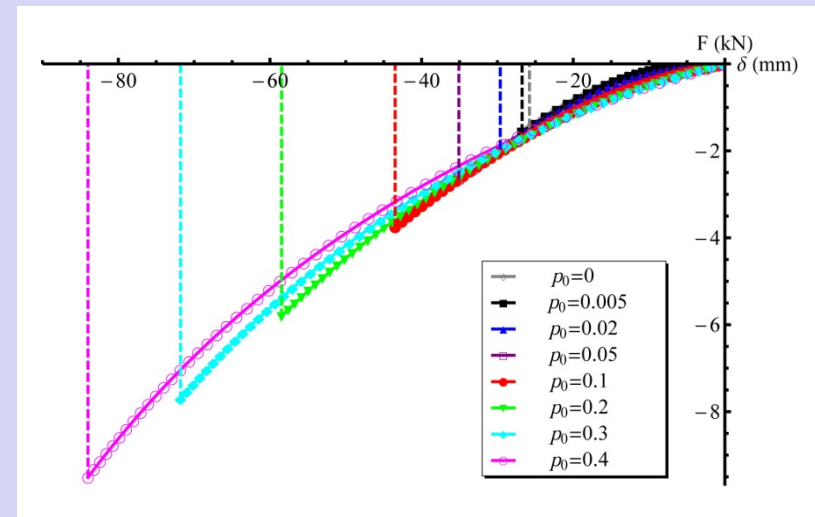
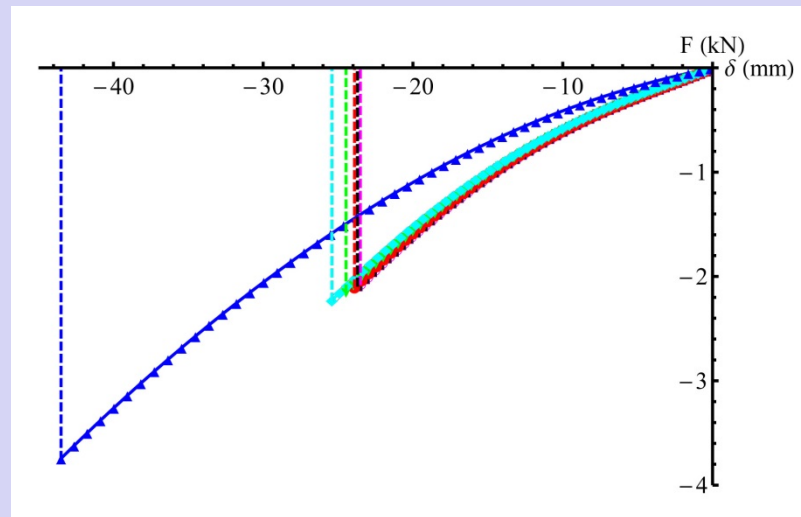
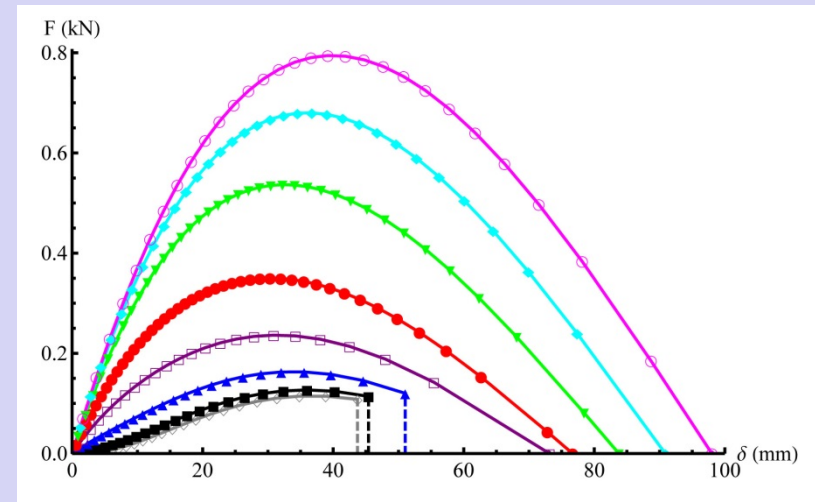
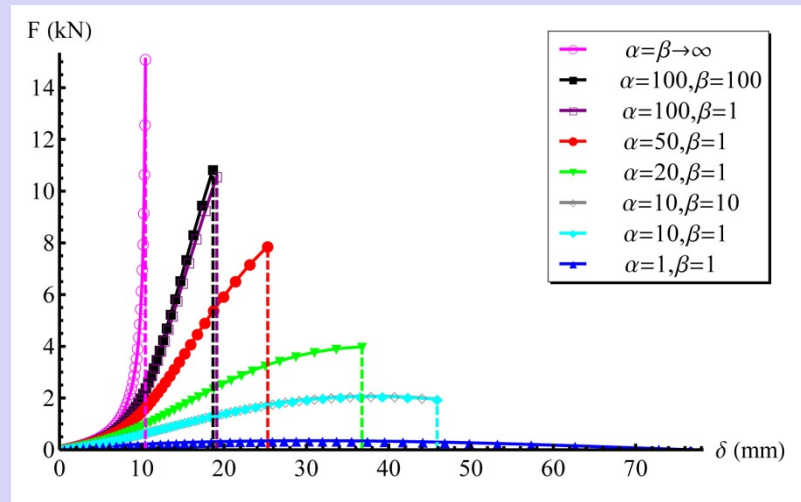
$$h = \sqrt{b^2 - \frac{2}{3}\ell^2(1 - \cos \varphi)} \quad \Longrightarrow \quad \varphi = \arccos \left(1 - \frac{b^2 - h^2}{2a^2} \right)$$

$$\begin{aligned} F &= 3k_1 (s - s_N) \frac{h}{2s} \left(3 + \frac{\sqrt{3}(2a^2 + h^2 - b^2)}{a^2 \sqrt{-\frac{(h^2 - b^2)(4a^2 + h^2 - b^2)}{a^4}}} \right) \\ &= \frac{k_1 \csc(\varphi) (3 \sin(\varphi) + \sqrt{3} \cos(\varphi)) \sqrt{3b^2 + 2\ell^2 \cos(\varphi) - 2\ell^2}}{2\sqrt{3b^2 - \sqrt{3}\ell^2 \sin(\varphi) + 3\ell^2 \cos(\varphi)}} \\ &\quad \times \left(\sqrt{9b^2 - 3\sqrt{3}\ell^2 \sin(\varphi) + 9\ell^2 \cos(\varphi) - 3s_N} \right) \end{aligned}$$

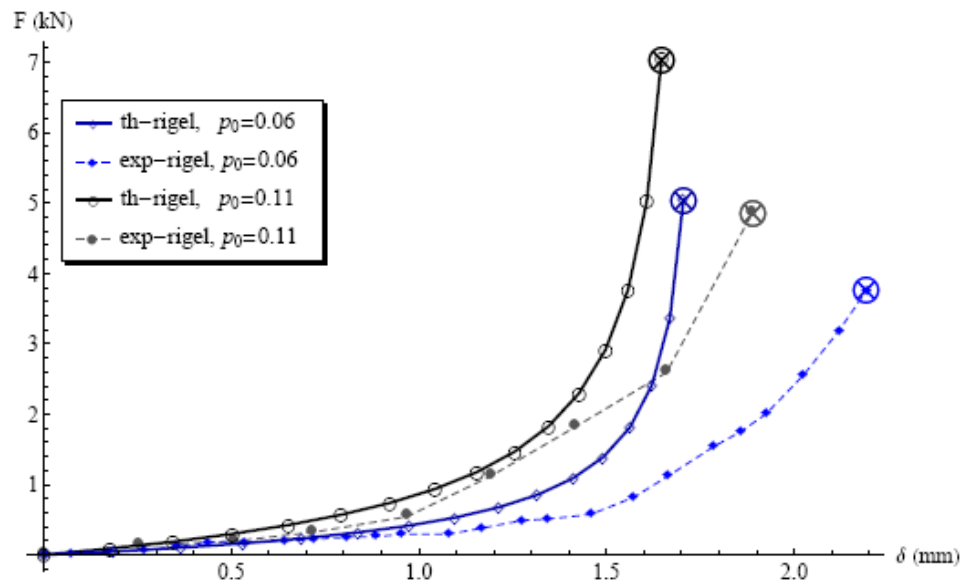
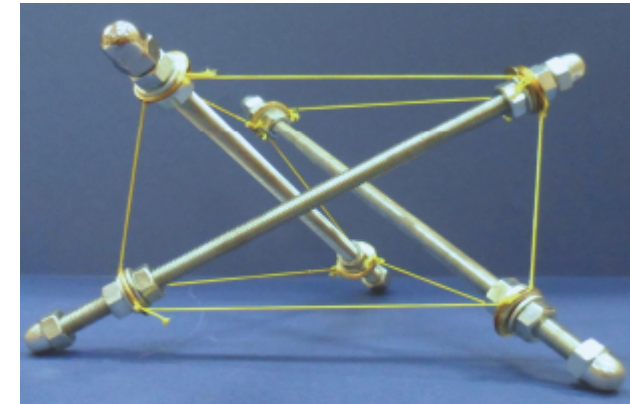
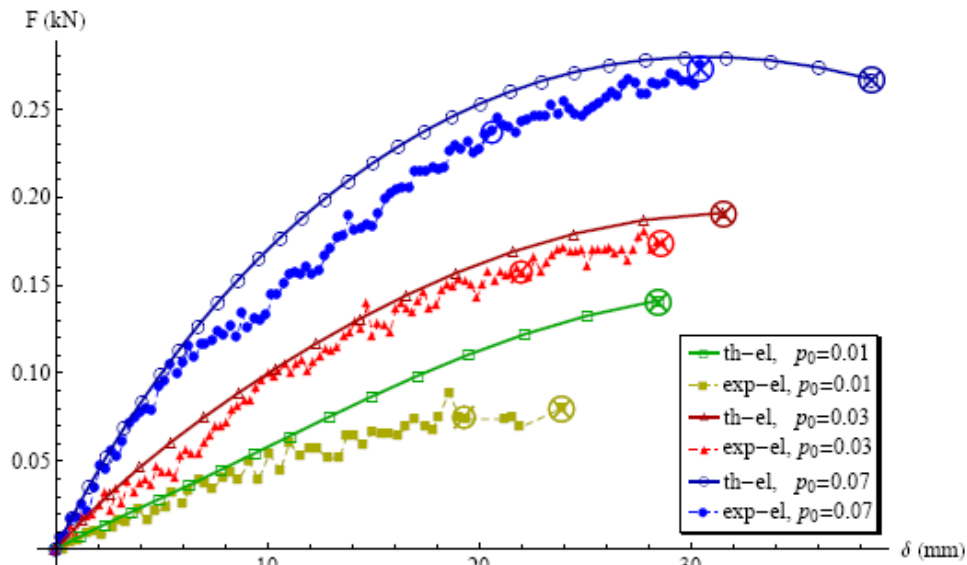
Force-displacement response of a rigid-elastic prism



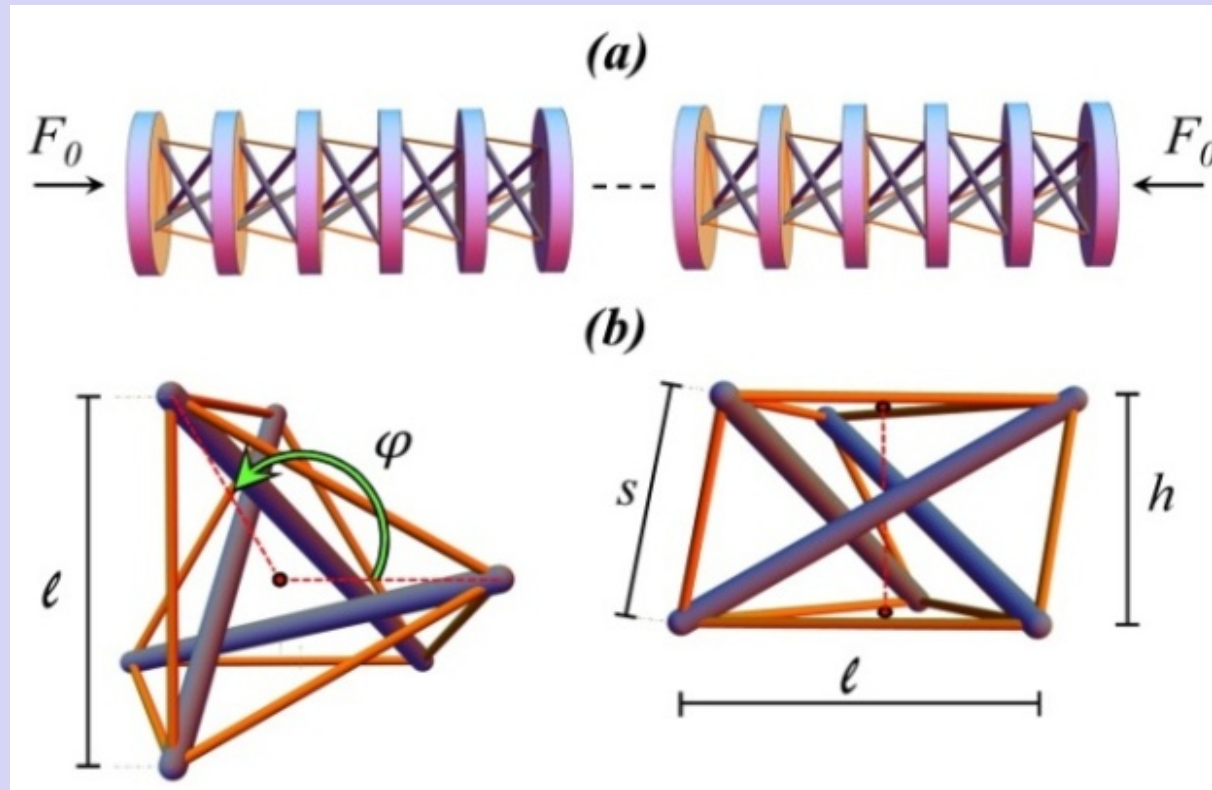
Effects of element rigidity and internal prestress



Experimental validation of the constitutive response



Tensegrity metamaterials



(a) Chain of tensegrity prisms (strongly nonlinear springs) and lumped masses globally prestressed by force F_0 . (b) Top view (on the left) and side view (on the right) of the tensegrity unit.

Properties of the elastic potential of rigid-elastic prisms

- (H1) *minimum at zero*: $V \in C^3(-d, \infty)$, $V \geq 0$, $V(0) = 0$, $V''(0) > 0$;
- (H2) *growth*: $V(r) \geq c_0(r+d)^{-1}$, for some $c_0 > 0$ and all r close to $-d$;
- (H3) *hardening*: $V'''(r) < 0$ in $(-d, 0]$, $V(r) < V(-r)$ in $(0, d)$.

For $c \approx c_s$, the continuum limits of the strain waves traveling on lattices endowed with such potentials have a small-amplitude profile of the form $\varepsilon_c(x) = \varepsilon_{\text{sech}^2}(x) + O(\gamma^4)$ (Friesecke and Pego, 1999), where x is a coordinate centered at the wave peak, and it results

$$\varepsilon_{\text{sech}^2}(x) = -\frac{a}{bh_0} \left(\frac{\gamma}{2} \operatorname{sech} \left(\frac{\gamma x}{2h_0} \right) \right)^2$$

with

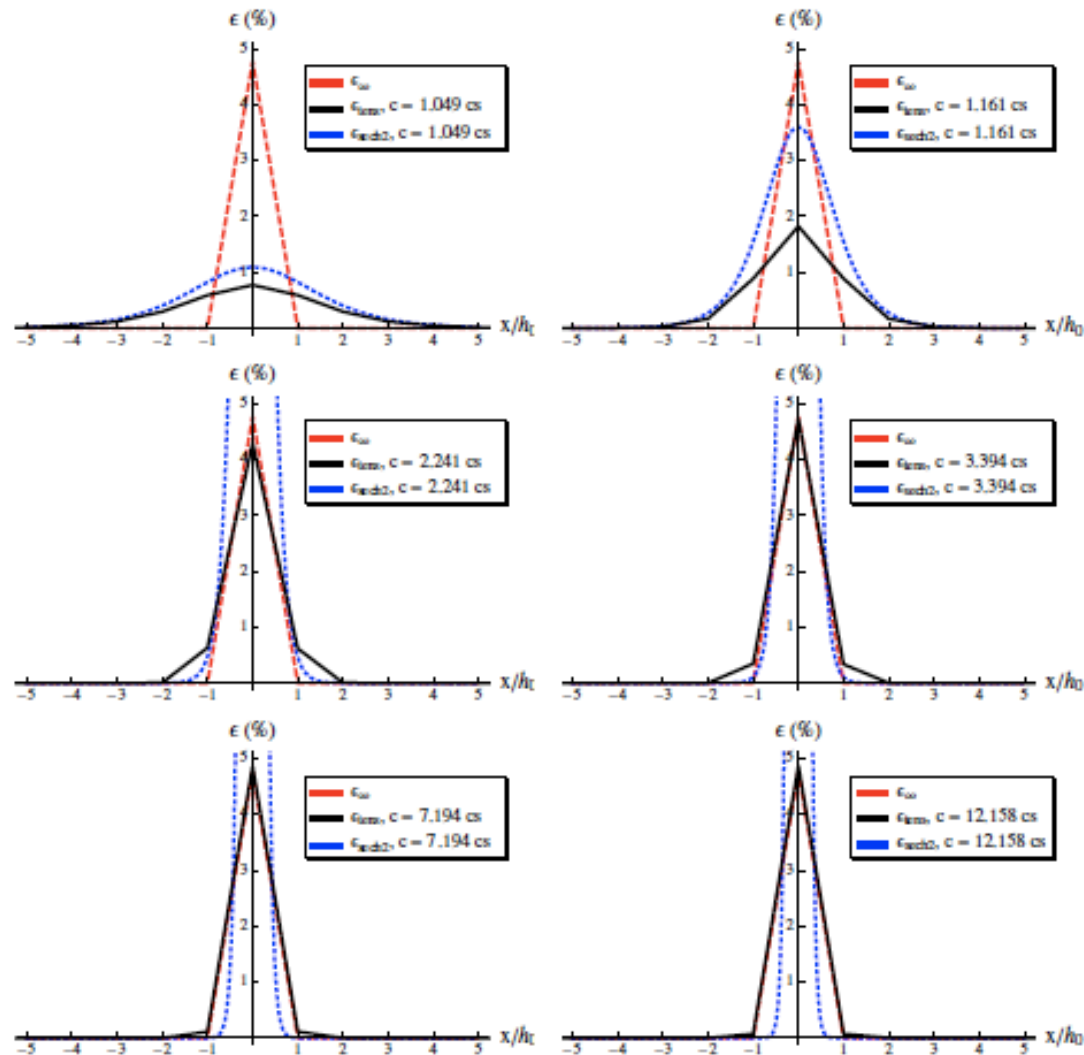
$$\gamma^2 = 24 \frac{c - c_s}{c_s}, \quad a = V''(0), \quad b = V'''(0)$$

$$c_s = h_0 \sqrt{\frac{V''(0)}{m}}$$

h_0 denoting the lattice spacing. Differently, for $c \gg c_s$ (that is, $c \rightarrow \infty$), the strain waves tend to assume a piecewise linear profile $\varepsilon_\infty(x)$, which is concentrated on a single lattice spacing and defined as follows (Friesecke and Matthies, 2002):

$$\varepsilon_\infty(x) = \begin{cases} 0 & \text{if } x/h_0 \leq -1 \\ d/h_0 (1 - |x/h_0|) & \text{if } x/h_0 \in [-1, 1] \\ 0 & \text{if } x/h_0 \geq 1 \end{cases}$$

Numerical simulation



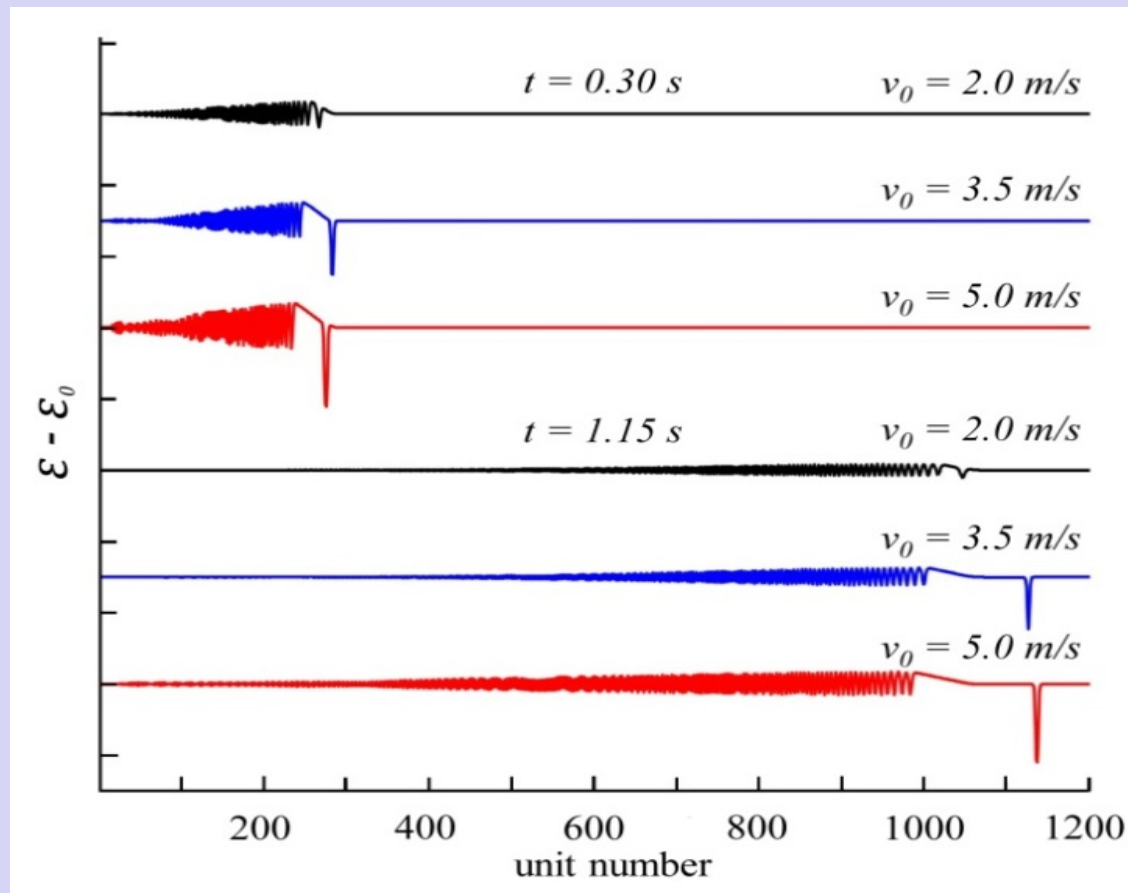
We observe a good matching between ϵ_{sech}^2 and ϵ_{tens} for $c \approx 1.05 c_s$.

$\epsilon_{tens}(x)$ is localized on about 7 prisms for $c = 1.05 c_s$; and 3 prisms for $c = 2 \div 3 c_s$.

$\epsilon_{tens}(x)$ almost coincides with the supersonic profile for $c = 12.16 c_s$.

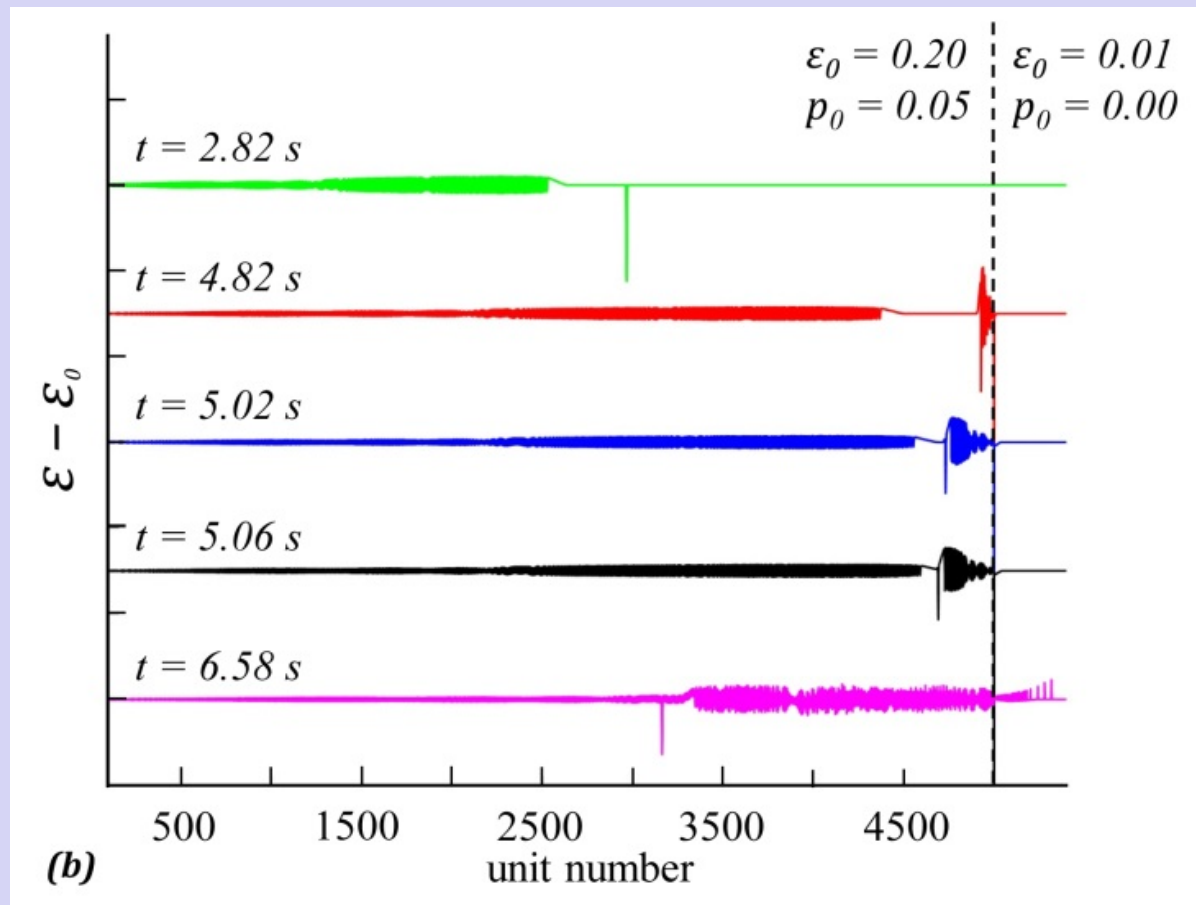
Rarefaction solitary waves on softening tensegrity lattices

The wave dynamics of lattices showing tensegrity units supports the formation of a leading rarefaction soliton followed by a dispersive, oscillatory tail. The rarefaction soliton moves at supersonic speed while the oscillatory tail moves at subsonic speed.



Composite hard-soft systems

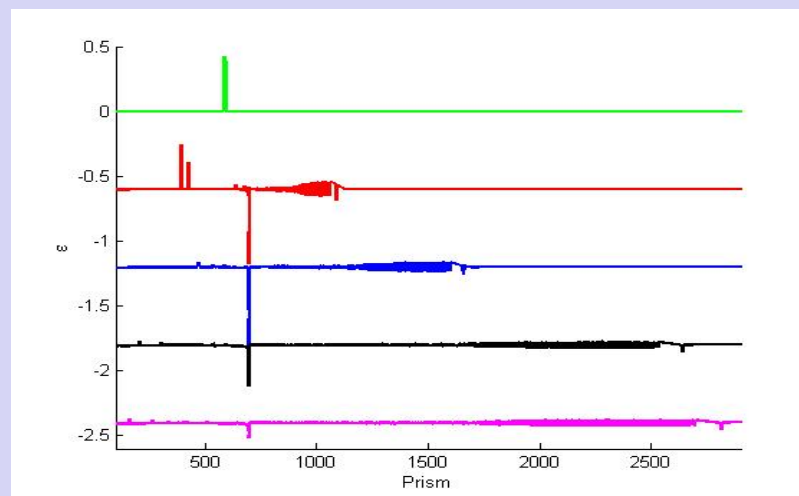
The interaction of a rarefaction solitary wave with an acoustically hard-soft interface also demonstrated anomalous behavior; a reflected solitary rarefaction wave with oscillatory tail in the acoustically hard branch; and a delayed train of transmitted compression solitary pulses in the acoustically soft branch..



Technical applications

The presented results highlight that softening tensegrity metamaterials may transform an initially compressive disturbance into a rarefaction wave of finite amplitude with progressively vanishing oscillatory tail. We demonstrated anomalous reflection of compression and rarefaction solitary waves from interfaces of two tensegrity based metamaterials.

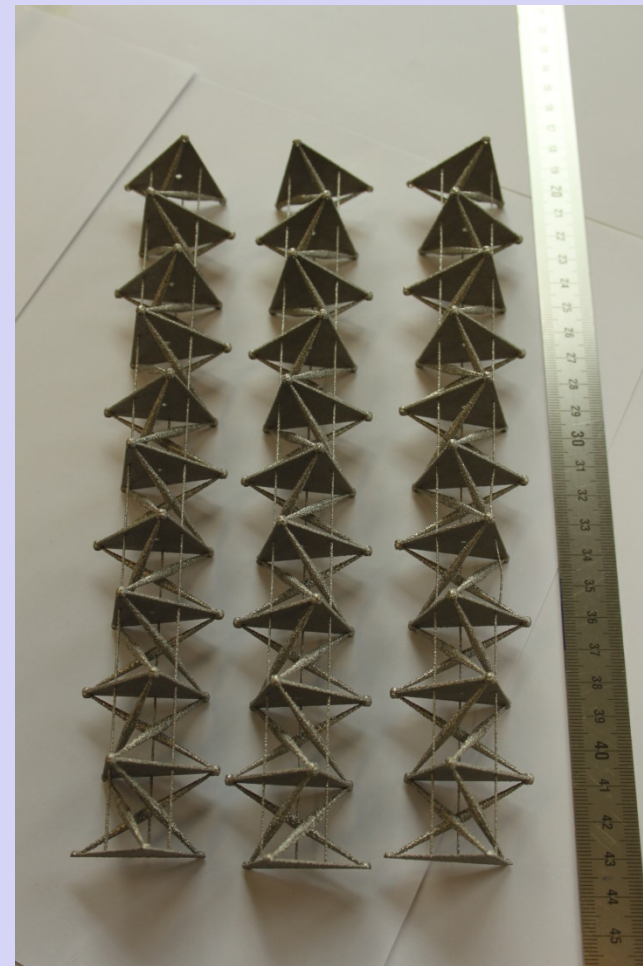
The analyzed systems can act as effective impact mitigation systems which do not require dissipation of energy, but a sufficiently large number of units, as a function of local and global prestress. If the size of the units can be scaled down to about $10\ \mu$, we expect that an effective impact protection barrier would require a total length of 1 cm.



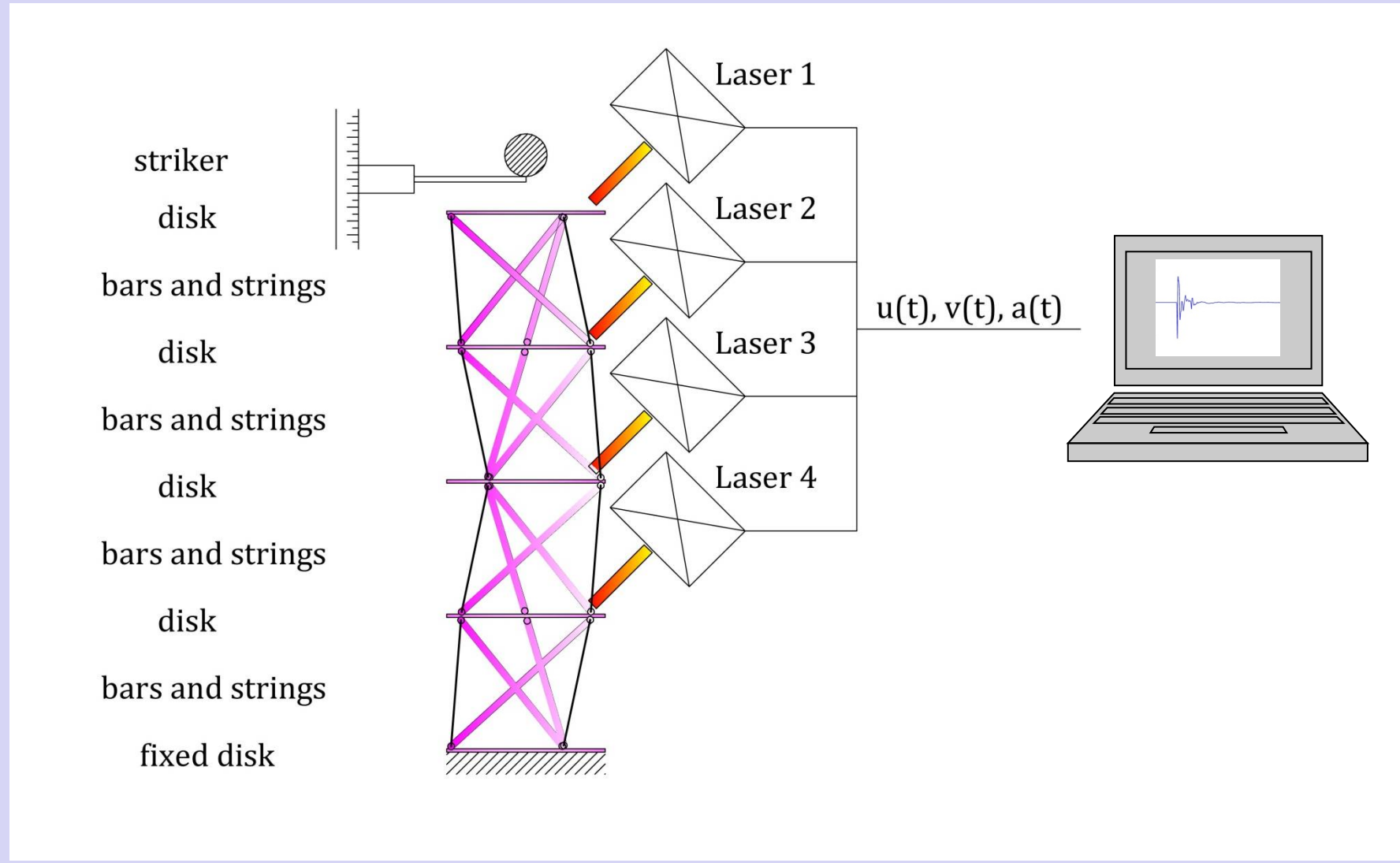
3D printing of titanium physical samples

(in collaboration with the Mercury Centre for Advanced Manufacturing Technology & Production, University of Sheffield, UK)

Ti6Al4V tensegrity prisms and columns



Experimental setup for dynamic tests on tensegrity chains (in progress)



Ongoing work

Generalize the mathematical work available in literature. on the existence and asymptotic profiles of localized waves on lattices with Lennard-Jones type interactions to softening lattices.

Design by computation of tensegrity metamaterials featuring a variety of behaviors not found in natural materials, such as, e.g., sound focusing; rarefaction waves; acoustic cloaking; wave-steering and stop-bands.

Main applications: acoustic lenses, innovative tools for nondestructive evaluation and monitoring of materials and structures; and shock absorption devices.